



HAL
open science

Ingestion of *Bacillus cereus* spores dampens the immune response to favor bacterial persistence

Salma Hachfi, Alexandra Brun-Barale, Arnaud Fichant, Patrick Munro, Marie-Paule Nawrot-Esposito, Gregory Michel, Raymond Ruimy, Raphaël Rousset, Mathilde Bonis, Laurent Boyer, et al.

► To cite this version:

Salma Hachfi, Alexandra Brun-Barale, Arnaud Fichant, Patrick Munro, Marie-Paule Nawrot-Esposito, et al.. Ingestion of *Bacillus cereus* spores dampens the immune response to favor bacterial persistence. Nature Communications, 2024, 15 (1), pp.7733. 10.1038/s41467-024-51689-9 . hal-04688484

HAL Id: hal-04688484

<https://hal.univ-cotedazur.fr/hal-04688484>

Submitted on 5 Sep 2024

HAL is a multi-disciplinary open access archive for the deposit and dissemination of scientific research documents, whether they are published or not. The documents may come from teaching and research institutions in France or abroad, or from public or private research centers.

L'archive ouverte pluridisciplinaire **HAL**, est destinée au dépôt et à la diffusion de documents scientifiques de niveau recherche, publiés ou non, émanant des établissements d'enseignement et de recherche français ou étrangers, des laboratoires publics ou privés.



Distributed under a Creative Commons Attribution - NoDerivatives 4.0 International License








Ingestion of *Bacillus cereus* spores dampens the immune response to favor bacterial persistence

Received: 4 April 2024

Accepted: 13 August 2024

Published online: 04 September 2024

 Check for updates

Salma Hachfi ^{1,2}, Alexandra Brun-Barale¹, Arnaud Fichant^{1,3}, Patrick Munro², Marie-Paule Nawrot-Esposito¹, Gregory Michel ², Raymond Ruimy^{2,4}, Raphaël Rousset ¹, Mathilde Bonis³, Laurent Boyer ²  & Armel Gallet ¹ 


Strains of the *Bacillus cereus* (*Bc*) group are sporulating bacteria commonly associated with foodborne outbreaks. Spores are dormant cells highly resistant to extreme conditions. Nevertheless, the pathological processes associated with the ingestion of either vegetative cells or spores remain poorly understood. Here, we demonstrate that while ingestion of vegetative bacteria leads to their rapid elimination from the intestine of *Drosophila melanogaster*, a single ingestion of spores leads to the persistence of bacteria for at least 10 days. We show that spores do not germinate in the anterior part of the intestine which bears the innate immune defenses. Consequently, spores reach the posterior intestine where they germinate and activate both the Imd and Toll immune pathways. Unexpectedly, this leads to the induction of amidases, which are negative regulators of the immune response, but not to anti-microbial peptides. Thereby, the local germination of spores in the posterior intestine dampens the immune signaling that in turn fosters the persistence of *Bc* bacteria. This study provides evidence for how *Bc* spores hijack the intestinal immune defenses allowing the localized birth of vegetative bacteria responsible for the digestive symptoms associated with foodborne illness outbreaks.

Organisms are subjected to various environmental stresses including starvation, temperature variation, chemicals, and microbes. Healthy individuals overcome these assaults by engaging defense mechanisms that maintain their homeostasis. Among the stressors, opportunistic enteric bacteria become pathogenic when host defenses are diminished or inefficient.

The evolutionarily conserved innate immune system is the first line of defense against bacteria, and adult *Drosophila* has proven to be a powerful model for innate immunity studies¹. In the midgut, the local innate immune system is mainly mounted in the anterior parts^{1,2}. First, anterior enterocytes can rapidly sense the presence of allochthonous

(i.e., non-commensal) bacteria and secrete reactive oxygen species (ROS) in a DUOX-dependent manner to block bacterial proliferation^{3,4}. Concomitantly, luminal ROS are perceived by a subpopulation of anterior enteroendocrine cells that respond by releasing the DH31/CGRP neuropeptide, which promotes visceral muscle spasms to provoke the expulsion of bacteria from the midgut in less than 4 h post-ingestion⁴. Nevertheless, if the load of allochthonous bacteria is higher and/or if the immune ROS and visceral spasms are insufficient to eliminate them, the allochthonous bacteria can start to proliferate, releasing muropeptides from the peptidoglycan (PGN), a bacterial cell wall component, that bind to the transmembrane and intracellular

¹Université Côte d'Azur, CNRS, INRAE, ISA, Sophia Antipolis, France. ²Université Côte d'Azur, Inserm, C3M, Nice, France. ³Anses (Laboratoire de Sécurité des Aliments), Université Paris-Est, Maisons-Alfort, France. ⁴Bacteriology Laboratory, Archet 2 Hospital, CHU, Université Côte d'Azur, Nice, France.

 e-mail: Laurent.BOYER@univ-cotedazur.fr; Armel.GALLET@univ-cotedazur.fr

immune receptors PGRP-LC and PGRP-LE, respectively^{5,6}. Consequently, the Immune deficiency (Imd)/NF- κ B pathway is activated, leading to the expression of anti-microbial peptides (AMPs) beginning 4–6 h post-ingestion^{7–10}. Because a prolonged activation of the local innate immunity is responsible for chronic inflammation which is detrimental for the individual, a robust negative feedback is turned on to tune down the Imd pathway once the bacteria are cleared¹⁰. For instance, the PGRP-SC1 & 2 and PGRP-LB amidases have been described as negative regulators of the Imd pathway mainly acting by digesting the extracellular PGN fragments and thus blocking the recognition process by the Imd pathway receptors^{6,11–13}. Altogether, these combined means of defense allow an efficient sensing and elimination of the allochthonous bacteria allowing the survival of the individual.

However, the detection of bacterial spores by the local innate immune system of the intestine and their elimination remains challenging for host organisms. Indeed, spores can resist many biological, chemical, or physical treatments^{14,15}. Among opportunistic bacteria, the widespread environmental spore-forming bacteria belonging to the *Bacillus cereus* (*Bc*) group are well-known worldwide food poisoning pathogens that cause diarrheal and/or emetic-type illnesses^{16,17}. *Bc* is the first cause of foodborne outbreaks (FBOs) in France^{18–20} and in Europe²¹. When nutrient-rich conditions are encountered, *Bc* spores can germinate, giving rise to vegetative cells which can even proliferate. Such favorable conditions are present in the small intestine of mammals, where it is assumed that spores are able to germinate and probably proliferate to ultimately trigger diarrhea due to the production of enterotoxins^{14,22}. In vitro experiments have indicated that *Bc* vegetative cells can be destroyed by the acidic pH of the stomach and the biliary salt of the duodenum while spores can resist^{22–27}. The effectiveness of the gut innate immune system to fight *Bc* vegetative cells has been demonstrated⁴. In contrast, nothing is known concerning the behavior and the fate of *Bc* spores in the intestine in vivo and the related immune response mounted by the host.

Here, thanks to in vivo studies in *Drosophila melanogaster*, we demonstrate that spores of *Bc* group can persist for at least ten days in the intestine and we could detect their germination only in the posterior part of the midgut. Next, we demonstrate that the spores do not trigger any detectable immune responses in the anterior parts of the *Drosophila* midgut. Once in the posterior midgut, germinated cells trigger the Imd immune pathway in a PGRP-LE-dependent manner. Strikingly, we found the amidases PGRP-SC1/2 and PGRP-LB, which are negative regulators of the Imd pathways, to be induced while the AMPs were repressed. In flies deficient in the PGRP-LE receptor, the cytosolic members of the Imd pathway or the PGRP-SC1/2 and PGRP-LB amidases, the persistence of the bacteria in midgut was reduced. Surprisingly, removing Relish, the NF- κ B-like transcription factor, downstream of the Imd pathway has no impact on bacterial persistence. However, the depletion of Dif, another NF- κ B-like transcription factor, together with Relish provided proof of a critical cooperation of both transcription factors in regulating *amidase* and *AMP* expressions in the posterior midgut and thus the bacterial clearance. Altogether, we provide evidence that spores belonging to the *Bc* group persist in the intestine when ingested as spores and escape the anterior immune response. Spores reach the posterior regions of the midgut where they germinate, and vegetative bacteria induce expression of amidases that act as negative regulators of the Imd pathway, dampening the production of AMPs, and consequently fostering the persistence of the bacteria.

Results

Spores of the *Bc* group persist in the *Drosophila* intestine

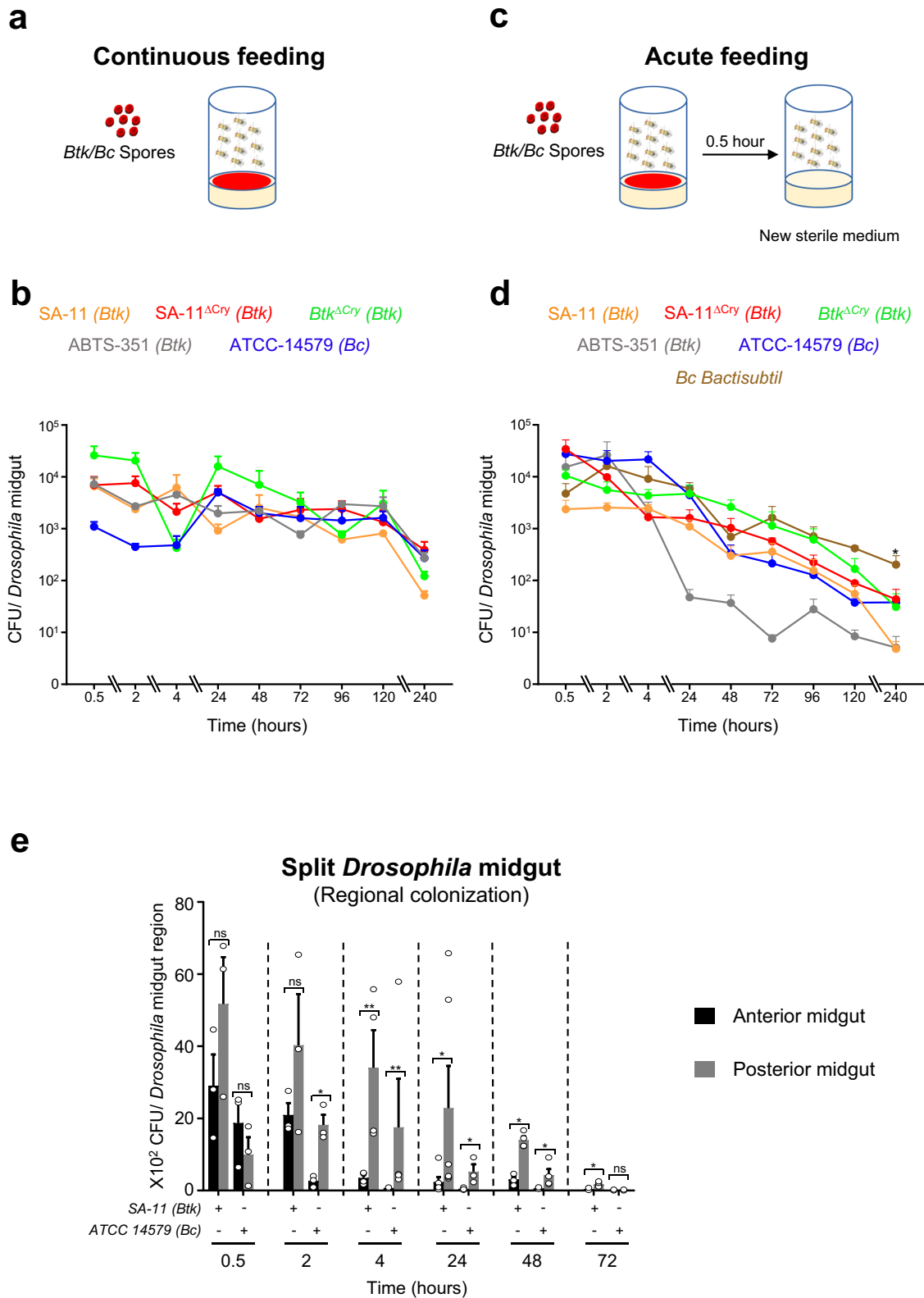
The *Bc* group is subdivided into at least eight phylogenetically very close genomospecies^{14,28,29}. For this study, we selected two *Bc sensu stricto* strains: the *Bc* ATCC 14579 type strain³⁰ and the probiotic strain,

Bc Bactisubtil, whose ingestion of spores have been used to alleviate gastrointestinal disorders³¹. We also selected two *Bacillus thuringiensis* subspecies *kurstaki* (*Btk*) strains (*Btk* SA-11 and *Btk* ABTS-351) because of their broad use as microbial pesticides and the fact that *Btk* has been suspected to be responsible for FBOs^{19,32,33}.

To determine whether, upon ingestion, *Bc* or *Btk* spores behaved the same as vegetative cells, we fed flies continuously with contaminated food (Fig. 1a) and assessed the amount of *Bc* or *Btk* bacteria in the *Drosophila* midgut at different times. We observed that regardless of the strain used, *Bc/Btk* were still present in the *Drosophila* midgut at least 10 days after the initial contact with spore-contaminated food (Fig. 1b). These data were very different from what we observed using *Bc* ATCC 14579 or *Btk* SA-11 vegetative cells, whose loads in the intestine rapidly decreased within 24 h (Fig. S1a). Unlike *Bc*, during sporulation, *Btk* produces Cry toxins embedded in a crystal, which displays specific entomopathogenic properties. *Btk* is widely used specifically to kill lepidopteran larvae that are broad crop pests¹⁴. Because the presence of Cry toxins might influence the behavior of *Btk* in the midgut, we engineered a *Btk* SA-11 ^{Δ Cry} strain cured of its plasmids and therefore devoid of Cry toxins (see Experimental Procedures). We also used a *Btk* ^{Δ Cry} obtained from the Bacillus Genetic Stock Center (#4D22, <https://bgsc.org/>) also devoid of Cry toxins. Importantly, the SA-11 ^{Δ Cry} and the *Btk* ^{Δ Cry} spores behaved like *Btk* SA-11 and *Bc* ATCC 14579 spores (Fig. 1b), refuting any possible role of the Cry toxins in *Btk* persistence. The commercially available preparation of the *Btk* ABTS-351 spores is known to contain 46% of additives (ec.europa.eu). To assess the potential involvement of those additives in the intestinal persistence of *Btk* ABTS-351, we extended our study to the commercial preparation, which we compared with a *Btk* ABTS-351 spore preparation made in our laboratory without any additives. We noticed that the commercial spores as well as the “homemade” *Btk* ABTS-351 spores behave similarly in the *Drosophila* midgut (Figs. 1b and S1b), suggesting that the additives present in the commercial preparation did not contribute to the persistence of *Btk* ABTS-351 spores.

Because spores could germinate and proliferate on the fly medium, we checked this possibility by counting the number of *Btk* SA-11 bacteria on the fly medium in the absence of flies. We applied a heat treatment in order to kill all germinated vegetative cells. We noticed that 2 days after spore deposit on the fly medium, some of them started their germination and even proliferated 4 days after deposit (Fig. S1c). Hence, to remove this limitation in the persistence assessment, we performed acute feeding. Flies were fed with spores for 30 min before being transferred onto fresh food medium (i.e. without spores) (Fig. 1c). We first verified that upon acute ingestion of *Bc* ATCC 14579 or *Btk* SA-11 vegetative cells, they were readily cleared from *Drosophila* midguts⁴ (Fig. S1d). We then monitored the persistence of spores in the *Drosophila* midgut upon acute feeding (Fig. 1d). We used 30 min of spore feeding as food intake internal control. At 30 min of spore feeding, the bacterial load averaged 10⁴ cells per midgut regardless of *Bc/Btk* strain. Interestingly, the bacteria could persist up to 10 days in the *Drosophila* midgut after acute spore ingestion (Figs. 1d and S1e). Noteworthy, we included the monitoring of the persistence of the probiotic *Bc* Bactisubtil strain and we found that *Bc* Bactisubtil load was significantly higher 10 days after acute feeding compared to all the other strains tested (Fig. 1d).

Because a recontamination of flies through their feces could occur during the 10 days of our experiments, we examined the amount of bacteria present in the feces and found only a small number of spores and vegetative cells (Fig. S1f). We also considered the potential for contamination by spores on the fly body during dissection. After examining fly bodies at 2, 24, and 48 h post-feeding, we found an average of 70 spores at 2 h, which decreased to 20 spores at 48 h (Fig. S1g). Our findings indicate that there is no evidence of contamination during the dissection or the reingestion of spores present



in the feces that could account for this persistence. We also observed that the bacterial persistence in the midgut was not dependent on the genetic background of *Canton S Drosophila* since similar amounts of bacteria were detected over the 10 days of monitoring in either *w¹¹¹⁸* or *w¹¹¹⁸* isogenic flies (Fig. S1h). Finally, the persistence was also not affected in axenic flies suggesting that the commensal flora does not influence the *Bc/Bt* intestinal persistence (Fig. S1h).

The *Drosophila* midgut is subdivided into five major anatomical regions (R1 to R5) (Fig. S1i)^{34,35}. To analyze in detail the localization of *Bc/Btk* along the midgut, we quantified the bacterial load in the anterior and posterior midgut after acute feeding. We did not focus on the acidic region due to its small size and the difficulty to dissect it accurately. During the first two hours after acute ingestion, we found that *Bc/Btk* bacteria were present in both regions of the midgut (anterior

Fig. 1 | Spores of the *Bacillus cereus* group persist in the *Drosophila* intestine. **a** Experimental setup to assess bacterial load after a continuous ingestion of spores. **b** Bacterial loads of dissected midguts after continuous ingestion of spores from *Btk* or *Bc* strains. The dot indicates the mean number of colony-forming units (CFUs) of at least three independent experiments per condition and time point. Each experiment corresponds to the mean of five midguts. CFUs correspond to spore and vegetative cell counts. Error bars correspond to the SEM. Source data are provided as a Source Data file. **c** Experimental setup to assess bacterial load after an acute ingestion of spores. Flies are in contact with the contaminated medium for 30 min and then transferred to fresh vial devoid of spores. **d** Bacterial loads of dissected midguts after acute ingestion of spores from *Btk* or *Bc* strains. The dot indicates the mean number of CFUs (spores + vegetative cells) of at least three

independent experiments per condition and time point. Each experiment corresponds to the mean of five midguts. Error bars correspond to the SEM. * represent statistically significant difference ($p < 0.05$) between *Bc* Bactisubtil and the other strains 10 days post-feeding using the two-sided Non-parametric Mann–Whitney test against each individual condition at 240 h. Source data are provided as a Source Data file. **e** Bacterial loads in split *Drosophila* midguts after acute intoxication with *Btk* (SA-11) or *Bc* ATCC 14579 spores. Dots correspond to independent experiments and are the mean of five pooled midgut domains. Error bars correspond to the SEM. The one-side Mann–Whitney tests were applied. Asterisks represent a statistically significant difference between bacterial loads in the anterior and the posterior midguts: ** $p < 0.01$, * $p < 0.05$. Source data are provided as a Source Data file.

and posterior). However, from 4 h onward, the posterior midgut harbored a significantly higher load of *Bc/Btk* cells compared with the anterior midgut (Fig. 1e). Collectively, our results demonstrate that *Bc/Btk* persist for up to 10 days in the midgut and may accumulate preferentially in the posterior regions.

Spores of the *Bc* group germinate preferentially in the posterior midgut

Spores are metabolically dormant and resistant to extreme environmental conditions, allowing them to survive to extreme conditions¹⁵. However, the presence of nutrients can trigger the process of germination, in which spores emerge from dormancy, growing into vegetative cells. Since the intestine is a favorable environment for spore germination, we hypothesized that *Bc/Btk* spores might germinate in the *Drosophila* midgut. To address this question, we developed a robust fluorescent staining technique suitable for visualizing spores and differentiating them from their outgrowing vegetative cells. Dormant *Bc/Btk* spores harbored a red fluorophore cross-linked to the spore outer membrane. Once germinated, vegetative cells started to express the green fluorescent protein (GFP). The use of this novel tool endowed with dual red/green (R/G) labeling allowed us to follow the process of germination in real-time (Fig. 2a and supplementary movie 1).

The use of the *Btk* SA-11^{RG} fluorescent strain in vivo first revealed that at 0.5- and 2-hours post-ingestion, *Btk* spores occupied the lumen of the whole midgut (Fig. S2a, b). Few vegetative cells were detectable in the posterior midgut 2 h post-ingestion (inset in Fig. S2b). *Btk* SA-11^{RG} spore germination was evident in the posterior midgut 4 h after ingestion (Fig. 2b, c). Interestingly, we found that regardless of the *Bc* group strain, excepted *Bc* Bactisubtil, spore germination occurred markedly in the *Drosophila* posterior midgut at 4 h after ingestion (Fig. S2d). Twenty-four hours post-ingestion, we detected mostly vegetative cells in the posterior midgut (Fig. S2c). Noteworthy, very few germinated cells were observed for *Bc* Bactisubtil 24 h post-acute feeding (Fig. S2d). To further confirm that spores mainly germinated in the posterior midgut, we performed measurements of colony-forming units (CFUs) in the anterior and posterior parts of the midgut by comparing heat-treated intestinal samples (to kill germinating spores and vegetative cells but not spores) to non-heat-treated samples (cumulating spores, germinating spores and vegetative cells). Interestingly, we did observe in the anterior midgut region the almost exclusive presence of *Bc/Btk* spores, even 3 days after acute ingestion (Fig. 2d). However, in the posterior midgut, we observed the appearance of the first *Bc/Btk* germinating spores as early as 30 min after ingestion (Fig. 2e). Together, these results demonstrate that the germination of *Bc* group spores begins 30 min after oral ingestion and occurs mainly in the posterior midgut of *Drosophila melanogaster*.

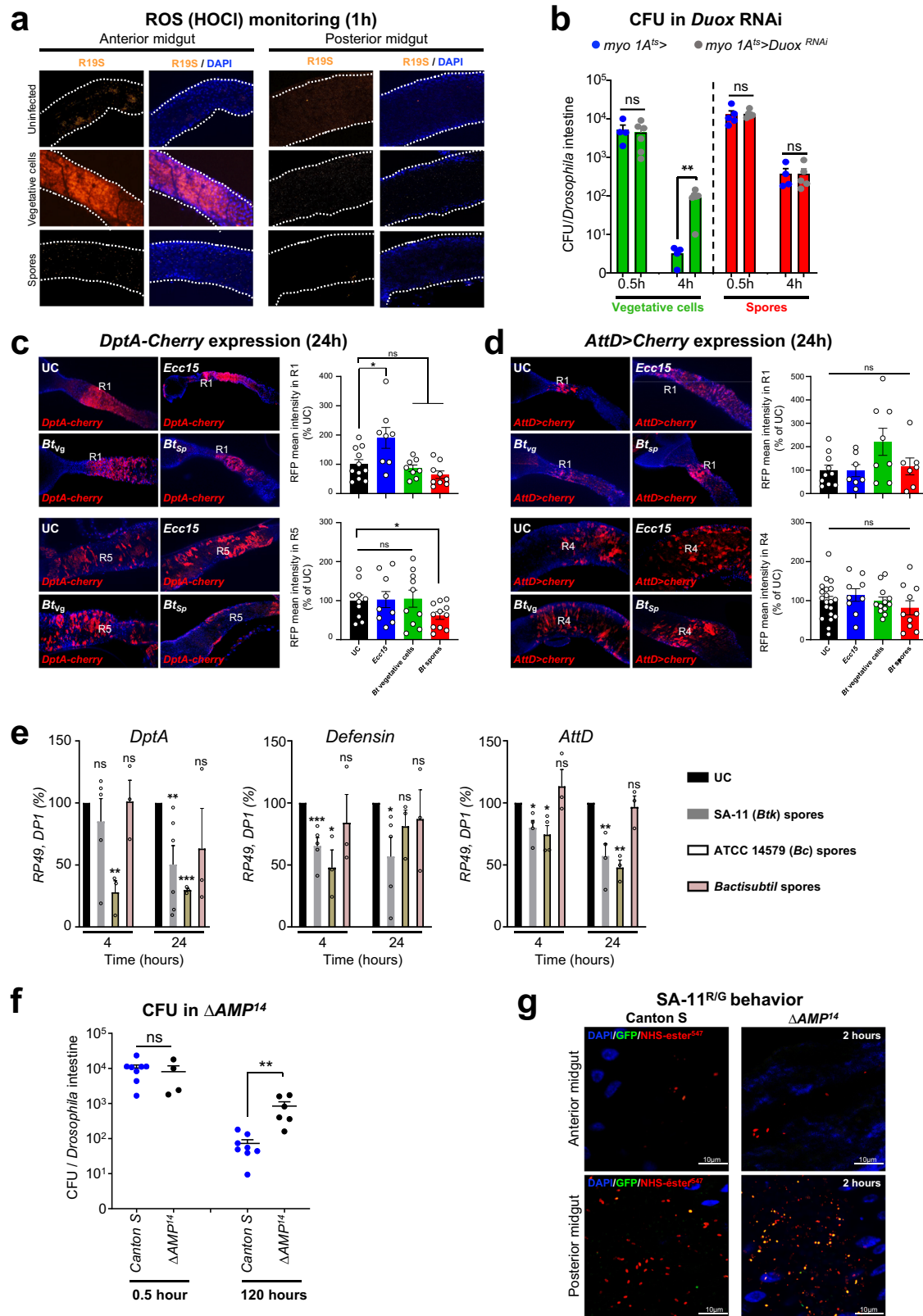
Spores do not trigger detectable *Drosophila* midgut innate immune response

The persistence of spores in the *Drosophila* midgut raises the question of how the local innate immune system can tolerate spores and/or

vegetative cells. As mentioned previously, in response to enteric infection, the anterior *Drosophila* midgut (R1 and R2 regions) initiates immune responses via the luminal release of ROS and, if necessary, AMPs^{2,4,5,36–38}. To test the release of local immune ROS (HOCl) in response to *Btk* vegetative cells or spores, we used the R19S probe, a HOCl sensitive fluorescent dye^{38,39}. First, we confirmed that *Btk* vegetative cells induced ROS only in the anterior region 1-hour post-ingestion (Fig. 3a, middle panel). Surprisingly, *Drosophila* fed with *Btk* spores did not show ROS induction either in the anterior or in the posterior regions of the *Drosophila* midgut at that time (Fig. 3a, lower panel), though spores germinated in the posterior midgut (Fig. 2 and S2). We investigated the potential ROS production at later time points (i.e. 4, 8 and 24 h) in the posterior midgut and no HOCl production was detected (Fig. S3a). In parallel, we specifically knocked down the expression of *Duox* in *Drosophila* enterocytes by RNA interference and examined the resulting impact on the spore persistence. We first confirmed that, 4 h after ingestion of vegetative cells, the silencing of *Duox* in the enterocytes increased the load of *Btk* compared with control intestines⁴ (Fig. 3b). However, *Duox* silencing in *Drosophila* enterocytes did not impact the *Btk* persistence after spore ingestion (Fig. 3b). Based on these data, we inferred that ingestion of spores does not induce the production of *Duox*-dependent ROS.

We next investigated the induction of AMP genes in the *Drosophila* midgut following acute ingestion of vegetative cells vs. spores. Using the *DiptericinA-Cherry* (*DptA-Cherry*) and *AttacinD-Gal4 UAS-Cherry* (*AttD>Cherry*) reporters, two readouts for the activation of the *lmd* pathway in the midgut⁴⁰, we first observed that the acute ingestion of vegetative cells of the *Erwinia carotovora carotovora* (*Ecc15*) opportunistic bacteria-induced *DptA* and *AttD* expression in the anterior midgut (Figs. 3c and S3b, c). *Ecc15* was also capable of promoting the spreading of *AttD* expression in the posterior R4 region (Fig. S3c). However, *Btk* vegetative cells did not show significant changes in *DptA* and *AttD* expression in either the anterior or posterior midgut (Figs. 3c, d, and S3b, c). These data are consistent with the fact that early ROS induction followed by the visceral spasms are sufficient to rapidly eliminate *Btk* vegetative cells upon acute ingestion (Fig. 3a, b)⁴, at least before the *lmd* pathway can be induced. RT-qPCR analyses of the expression of *DptA*, *Defensin*, and *AttD* genes on dissected midguts confirmed the non-induction of AMP genes after acute ingestion of *Btk* (or *Bc*) vegetative cells (Fig. S3d).

Monitoring AMP expression upon acute spore feeding revealed that neither *DptA-Cherry* nor *AttD>Cherry* reporter genes were induced in vivo in the anterior midgut (Figs. 3c, d and S3b, c). Strikingly, repression of the *DptA-Cherry* reporter expression in the posterior midgut was observed (Figs. 3c and S3b). RT-qPCR analyses confirmed the repression of *DptA* expression as well as the repression of *Defensin*, *AttD*, and *Drosomycin* (*Drs*) expression (Figs. 3e and S3e). Importantly, ingestion of *Bc* Bactisubtil spores that did not germinate in posterior in midgut (Fig. S2d) did not lead to the repression of AMP expression (Fig. 3e). This emphasizes the significance of localized spore germination in the posterior midgut, which is essential for promoting the down-regulation of AMP expression. Together these data suggest that



Bc/Btk persistence upon spore ingestion and germination in the posterior midgut could be supported by decreased expression of *AMPs*.

To assess the involvement of the *AMPs* in *Btk* SA-11 persistence, we used a fly strain in which the 14 *AMP* genes were deleted (ΔAMP^{14})^{41,42}. We quantified the *Btk* SA-11 load in the midgut of Wild Type (*Canton S*) and ΔAMP^{14} flies. While both genotypes ingested a similar amount of spores during the 30 min of feeding (Fig. 3f), 120 h post-

feeding, in ΔAMP^{14} mutant flies, we found a significantly higher *Btk* SA-11 load compared with wild-type flies (Fig. 3f). This result suggests that *AMPs* could kill germinating cells in the posterior midgut. To further challenge this hypothesis, we monitored the fate of the *Btk* SA-11^{R/G} fluorescent strain in ΔAMP^{14} mutant flies after acute ingestion of spores. Interestingly, as soon as two hours post-ingestion, confocal imaging showed higher levels of germinating spores in ΔAMP^{14} mutant

Fig. 3 | *Bc/Bt* spores do not trigger midgut innate immune response. **a** ROS monitoring one-hour post-acute feeding with SA-11 spores or vegetative cells. ROS production in the midgut is visualized by the HOCl-specific R19S probe (orange). DAPI (blue) marks the nuclei. **b** SA-11 loads in midguts knocked down for the expression of *Duox* in enterocytes 0.5 or 4 h after acute feeding with vegetative cells or spores. The horizontal axis indicates the mean number of CFUs. Dots correspond to independent experiments of five pooled midguts. **c** *DptA-Cherry* expression (red) in the anterior R1 midgut region (upper panel) and in the posterior R5 midgut region (bottom panel) of *Drosophila* fed for 30 min with H₂O, *Ecc15*, SA-11 vegetative cells (*Bt_{veg}*) or SA-11 spores (*Bt_{sp}*) and observed 24 h later. In each panel anterior is to the left. Measured quantities are shown on the right graphs. The results are given as the relative expression compared with the control (H₂O). At least three independent experiments were performed and each dot correspond to one midgut. **d** *AttD-Gal4 UAS-Cherry* expression (red, *AttD>Cherry*) in the anterior R1 midgut region (upper panel) and in posterior R4 midgut region (bottom panel) of *Drosophila* fed for 30 min with H₂O, *Ecc15*, SA-11 vegetative cells (*Bt_{veg}*), or SA-11 spores (*Bt_{sp}*) and observed 24 h later. Measured quantities are shown on the right graphs. The results are given as the relative expression compared with the control

(H₂O). At least three independent experiments were performed and each dot correspond to one midgut. **e** qRT-PCR analyses of *AMP* expression in midgut upon acute feeding with SA-11 or *Bc* spores. UC corresponds to flies fed with water. For RT-qPCR results, mRNA levels in unchallenged wild-type flies were set to 100 and all other values were expressed as a percentage of this value. RT-qPCR results are shown as mean ± SEM. Dots correspond to independent experiments of 10 pooled female flies. **f** Bacterial load in the midguts of Δ *AMP⁴⁴* mutant flies 0.5 or 4 h after acute feeding with SA-11 spores. The horizontal axis indicates the mean number of CFUs per midgut. Each dot corresponds to an independent biological replicate where each replicate is the mean of five midguts. **g** Representative confocal images showing SA-11^{RG} spore germination in the anterior and posterior midgut of WT (*Canton S*) and Δ *AMP⁴⁴* mutant flies 2 h after acute feeding with spores. DAPI (blue) marks the nuclei. Spores are in red, vegetative cells in green. The yellow fluorescence corresponds to germinating spores. Error bars correspond to the SEM. The two-sided Mann–Whitney test was applied in **b–d** and **f**. A two-sided Student's *t*-tests were used to analyze data in **e**. **p* ≤ 0.05, ***p* ≤ 0.01, ****p* ≤ 0.001, ns non-significant (exact *P* values are provided in the source data). Source data are provided as a Source Data file.

posterior midguts than in WT posterior midguts (Fig. 3g). We did not observe obvious changes in the anterior midguts where only spores were present (Fig. 3g). Collectively, our data suggest that, though repressed upon spore ingestion and their germination in the posterior midgut, the weak production of AMPs is necessary to limit the *Bc/Btk* bacterial load.

Amidases contribute to the intestinal persistence of spores

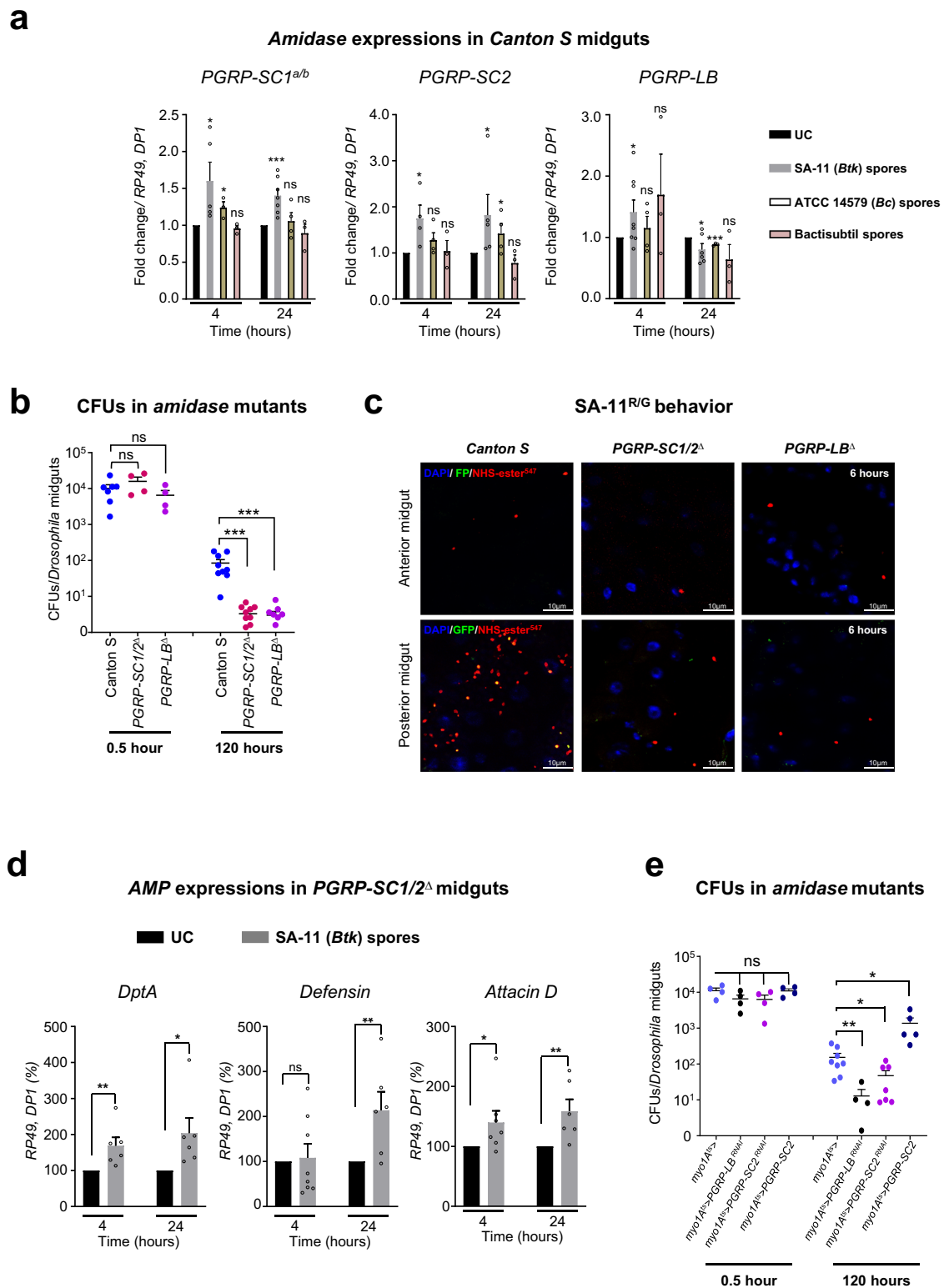
Since *AMPs* expression was downregulated after spore ingestion, we wondered whether the amidases, which exert negative feedback on the Imd pathway, could be induced by germinating spores^{11,12,40}. First, we verified by RT-qPCR analyses that the ingestion of *Bc/Btk* vegetative cells could induce the expression of the three *amidase* encoding genes in the midgut (Fig. S4). Interestingly, after spore ingestion, we observed that *PGRP-SCI* and *-SC2* were consistently induced both 4 h and 24 h post-feeding while *PGRP-LB* was only induced at 4 h and was repressed at 24 h (Fig. 4a). Noteworthy, *Bc Bactisubtil* did not induce any amidases confirming that the germination of spores in the posterior compartment is required to modulate Imd target genes (Fig. 4a). We next assessed the *Btk* SA-11 intestinal load in mutant flies homozygous for either the *PGRP-SCI/2* or *PGRP-LB* loss-of-function alleles (*PGRP-SCI/2^Δ* and *PGRP-LB^Δ* respectively)¹². In midguts from these mutant animals, no difference in bacterial load was observed compared with control flies 30 min after spore feeding (Fig. 4b). However, 120 h post-feeding, the loss of *PGRP-SCI/2* or *PGRP-LB* was associated with a significant decrease in the number of *Btk* SA-11 in the midgut compared with the WT flies (Fig. 4b). Because spores accumulated and germinated in the posterior midgut of WT flies as early as 4 h post-ingestion (Fig. 2), we monitored the fate of the spores in *PGRP-SCI/2^Δ* and *PGRP-LB^Δ* deficient flies. Six hours after acute ingestion, confocal imaging showed the presence of fewer red/green germinating spores in the posterior midguts of *PGRP-SCI/2^Δ* or *PGRP-LB^Δ* flies compared with WT flies (Fig. 4c), suggesting that in the absence of amidases, the production of AMPs was able to kill germinating spores.

We therefore investigated whether the repression of *AMPs* expression upon spore ingestion was indeed dependent of amidases. As expected, expression of *AMPs* was not repressed; indeed, it was even induced by *Btk* SA-11 spore ingestion in a *PGRP-SCI/2^Δ* or *PGRP-LB^Δ* mutant background (Fig. 4d compared with 3e). Because amidases can be produced by the enterocytes or by the fat body (a systemic immune tissue) and can act at a distance from the site of production⁴⁰, we specifically silenced *PGRP-SC2* or *PGRP-LB* in enterocytes and, while food intake was not affected after the 30 min of feeding, we found a significant decrease in the load of *Btk* SA-11 in the midgut 120 h post-feeding (Fig. 4e). Conversely, the overexpression of *PGRP-SC2* in enterocytes resulted in an increased bacterial load 120 h post-feeding

without any effect on food intake measured after 30 min (Fig. 4e). Overall, our data suggest that spores are not detected by the anterior midgut immune response (i.e., no production of ROS or AMPs), and reach the posterior regions where they germinate and can activate the Imd signaling target genes *PGRP-SCI*, *PGRP-SC2*, and *PGRP-LB*. In turn, amidases promote a repression of the basal expression of AMP-encoding genes. Consequently, downregulation of *AMP* expression favors *Bc/Btk* persistence in the posterior *Drosophila* midgut.

The Imd pathway contributes to the intestinal persistence of bacteria

Because the expression of *amidases* is under the control of the Imd pathway in the intestine, we first tested the involvement of the two Imd pathway receptors, *PGRP-LC* and *-LE*, in *Btk* SA-11 persistence. In flies homozygous viable for the loss-of-function mutant for either receptor, similar amounts of *Btk* SA-11 were ingested compared with WT flies after 30 min of spore feeding (Fig. 5a). Nevertheless, 120 h after feeding, only *PGRP-LE¹²* mutant flies showed a significant decrease in *Btk* SA-11 intestinal load (Fig. 5a) similar to that observed for flies lacking the amidases (Fig. 4b). We further tested mutants for intracellular components of the Imd pathway. Loss-of-function mutants for the cytoplasmic components Imd (*ima^{Shaddock}*) or Dredd (*Dredd^{f64}*) also displayed a decrease in *Btk* SA-11 persistence 120 h post-ingestion (Fig. 5a). Unexpectedly, the bacterial load in flies homozygous mutant for the downstream Imd pathway NF-κB-like transcription factor Relish (*Rel^{E20}*)⁴³ was similar to control flies (Fig. 5b), although Rel has been found to be absolutely required in midgut epithelial cells to respond to enteropathogenic bacteria^{5,8,44}. To further understand the apparent absence of *Rel* function in our model of spore infection, we inhibited *Relish* expression specifically in enterocytes. Silencing *Relish* in enterocytes did not change *Btk* bacterial abundance in the midgut (Fig. 5b). In addition, we monitored the fate of the *Btk* SA-11^{RG} fluorescent strain in *Rel^{E20}* mutants, six hours after acute ingestion. No obvious differences between WT and *Rel^{E20}* were observed in the *Drosophila* midgut (Fig. 5c). We also performed an epistasis experiment, removing both *PGRP-SCI* and *-SC2* amidases in the *Rel^{E20}* loss of function background. Interestingly, while food intake measured after 30 min was not affected, the bacterial load was lower 120 h post-feeding compared with the control (Fig. 5b) to a similar extent to that of mutants for *amidases* alone (Fig. 4b). This observation suggests that amidases act downstream of Relish to control *Btk* persistence. Finally, we overexpressed in enterocytes an activated form of Relish known to strongly induced *AMP* expression⁴⁵. As expected, we observed a reduced bacterial load 120 h after spore ingestion (Fig. 5b). Together, these data suggest that Relish has no significant role in the control of *amidase*



expression in the posterior midgut and that *Btk* persistence depends on finely-tuned expression levels of *amidases* and *AMPs*.

Given these observations, we wanted to test the involvement of Relish in controlling the remaining *AMP* expression in WT flies fed with spores (Fig. 3e). In *Rel^{E20}* unchallenged flies, while *DptA* and *Defensin* were drastically downregulated, *Attacin* expression was not affected (Fig. S5a). In addition, still in unchallenged flies, the absence of Relish correlated with the downregulation of *PGRP-SC1a/b* and *PGRP-LB* expression but, unexpectedly, *PGRP-SC2* was strongly upregulated

(Fig. S5b). Hence, the above data suggest that Relish is involved in the repression of *PGRP-SC2* expression and is not necessary for the basal *AttD* expression.

We further investigated the midgut expression of *AMPs* and *amidases* in a *Rel^{E20}* mutant background upon spore ingestion. The expression of *AMPs* was neither induced nor repressed (as one would have expected since spore feeding induced *AMP* repression in a wild-type background, Fig. 3e) 4 h or 24 h post-feeding with spores (Fig. 5d). Even though *PGRP-SC2* expression remained high, the expression of

Fig. 4 | Amidases are involved in *Bt/Bc* persistence. **a** qRT-PCR analyses of *amidase* expressions in midguts upon SA-11 or *Bc* spore acute feeding. UC corresponds to flies fed with water. Results are shown as mean \pm SEM. The dots correspond to independent experiments of 10 pooled female flies. **b** Bacterial load in midguts of *PGRP-SCI/2^d* double mutant or *PGRP-LB^{dE}* mutant 0.5 or 120 h after SA-11 acute feeding with spores. The horizontal axis indicates the mean number of CFUs per midgut. Each dot corresponds to an independent biological replicate where each replicate is the mean of five midguts. **c** Representative confocal images showing SA-11^{R/G} spore germination in the anterior and posterior midgut of WT (*Canton S*), *PGRP-SCI/2^d* double mutant or *PGRP-LB^{dE}* mutant flies 6 h after spore acute feeding. DAPI (blue) marks the nuclei. Spores are in red, vegetative cells in green. The yellow fluorescence corresponds to germinating spores (Fig. 2a). **d** qRT-PCR analyses of *AMP* expressions in midguts of *PGRP-SCI/2^d* mutants following acute

feeding with SA-11 spores. UC corresponds to *PGRP-SCI/2^d* flies fed with water. mRNA levels in unchallenged *PGRP-SCI/2^d* flies were set to 100 and all other values were expressed as a percentage of this value. Results are shown as mean \pm SEM. Dots correspond to independent experiments of the mean of 10 pooled female midguts. **e** SA-11 load in midguts of flies silenced for *PGRP-SC2* or *PGRP-LB* or overexpressing *PGRP-SC2* specifically in enterocytes (using the *myo1A^{ts}* driver) 0.5 or 120 h after acute feeding with spores. The horizontal axis indicates the mean number of CFUs per midgut. Each dot corresponds to an independent biological replicate where each replicate is the mean of five midguts. Error bars represent SEM. Two-sided Student's *t*-tests were used to analyze data in **a** and **d**. Two-sided Mann-Whitney test was used to analyze data in **b** and **e**. **p* \leq 0.05, ***p* \leq 0.01, ****p* \leq 0.001, ns non-significant (*P* values are provided in the source data file). Source data are provided as a Source Data file.

amidases was not induced in *Rel^{E20}* mutants (Fig. 5e). Gathering these data suggests that *Btk* intestinal persistence is not affected upon spore ingestion by *Rel^{E20}* mutant flies because, first, the upregulation of *PGRP-SC2* likely compensates for the downregulation of *PGRP-SCI* and *-LB* and second, the normal level of *AttD* expression might be sufficient to limit *Btk* persistence, knowing that *AttD* expression was downregulated upon spore ingestion by WT flies (Fig. 3e).

Because in the absence of PGRP-LE receptor *Btk* load was lower 120 h after spore feeding (Fig. 5a), we wondered whether in *PGRP-LE¹²* loss of function mutant flies both the expressions of *AMPs* and *amidases* were impacted. In *PGRP-LE¹²* unchallenged flies, the expressions of *DptA*, *Defensin*, *PGRP-SCI* and *-SC2* were lowered while *AttD* and *PGRP-LB* expressions were unaffected (Fig. S5c, d). Upon feeding *PGRP-LE¹²* flies with spores, none of the *amidases* were induced (Fig. 5g) confirming that PGRP-LE is the primary receptor in the posterior midgut that regulates amidase expression⁵. Conversely, both *Defensin* and *AttD* were induced 4 h post-ingestion (Fig. 5f). Interestingly, though mild, this rise in *AMP* expression was correlated with the reduced bacterial load observed 120 h post-ingestion (Fig. 5a).

Taken together our data demonstrate that PGRP-LE is required to sense *Bc/Btk* geminating cells in the posterior midgut and consequently to activate the expression of the *amidases*. In turn, amidases provoke a reduction of *AMPs* expression by tuning down the Imd pathway but likely also by tuning down another pathway since *Defensin* and *AttD* are still induced by the ingestion of spores in absence of PGRP-LE. Consequently, the decrease in *AMP* levels favor the local *Bc/Btk* persistence in the posterior midgut.

Toll pathway participates to the regulation of *amidases* and *AMPs* in the posterior midgut in response to spore ingestion

The above data prompted us to investigate the possible involvement of the immune Toll signaling pathway in the *Drosophila* posterior midgut. The NF- κ B-related transcription factor, the Dorsal-related immunity factor (Dif), acts downstream of the Toll pathway during the systemic immune response^{46–49}. To understand whether Dif could also be involved in *Bc/Btk* persistence, we took advantage of flies homozygous viable for the *Dif* loss-of-function allele, *Dif¹*. While *Dif¹* and WT flies ingested similar amounts of spores during the 30 min of feeding, 120 h later, we observed a significant decrease of *Btk* SA-11 loads in *Dif¹* mutant flies (Fig. 6a). Confocal microscopy analysis confirmed the decrease of *Btk* SA-11^{R/G} fluorescent cells, primarily in the posterior midguts of *Dif¹* mutant flies, compared with WT (Fig. 6b). We confirmed the involvement of the Toll signaling pathway first by feeding *Myd88* loss of function flies with spores. *Myd88* is an adapter acting downstream of Toll receptor and upstream of Dif^{50,51}. Second, we specifically silenced *Toll* expression in enterocytes. In both mutants, the bacterial load was reduced 120 h after feeding with spores (Fig. 6a). To further analyze the role of the Toll pathway in the intestinal immune response, we monitored the midgut expression of *AMPs* and *amidases* in *Dif¹* or *Myd88* mutant flies by qRT-PCR. In uninfected flies, the expression of *DptA* and *Defensin* was significantly lowered in both

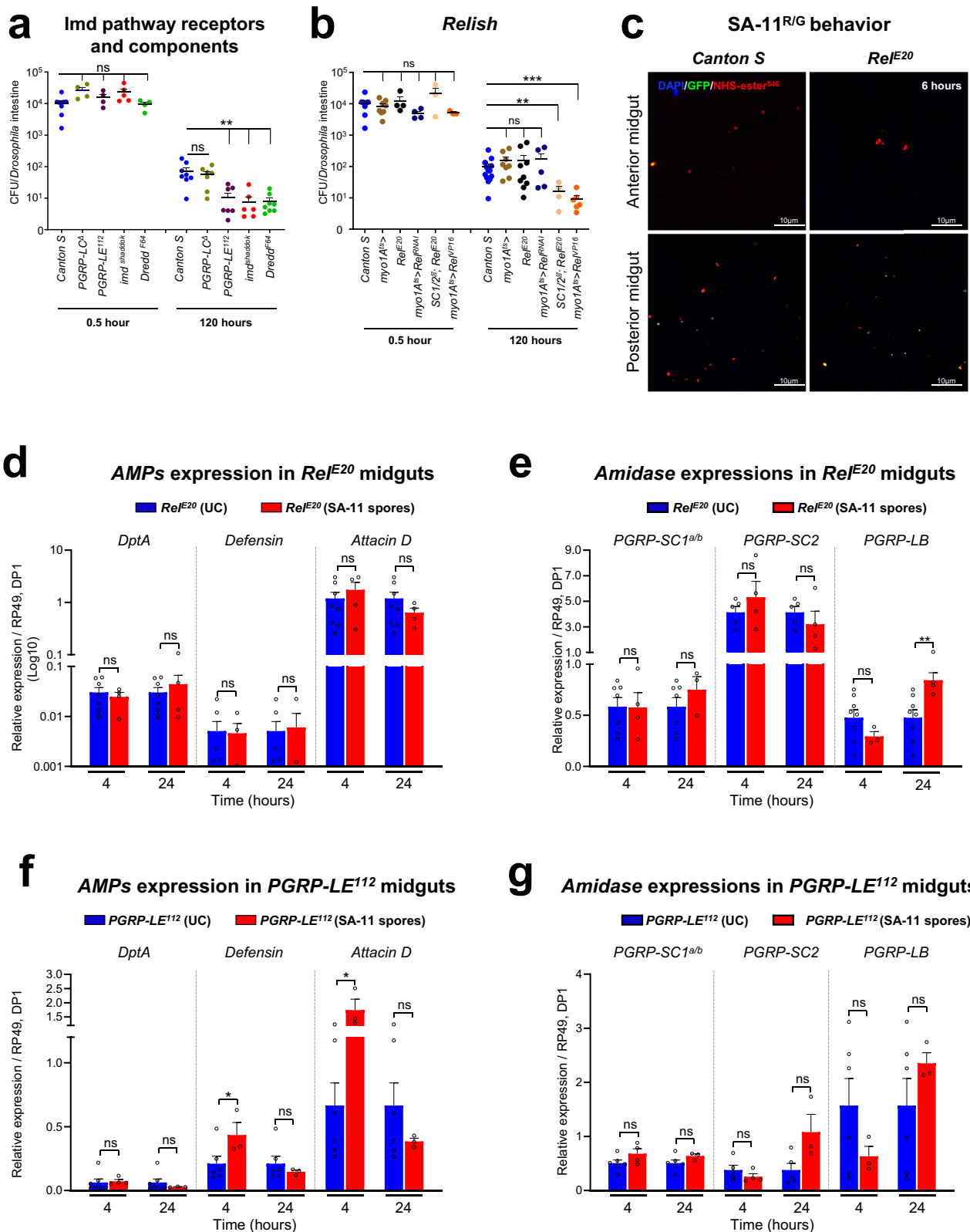
mutants compared with WT, while *AttD* was not affected (Fig. S6a, c). The expression of *PGRP-SC2* was also not affected in these mutants (Fig. S6b, d). Nevertheless, *PGRP-SCI* was downregulated in *Dif¹* mutant flies but upregulated in *Myd88* mutant flies (Fig. S6b, d). Finally, *PGRP-LB* expression was unaffected in *Dif¹* mutant flies but downregulated in *Myd88* mutant flies (Fig. S6b, d).

Feeding *Dif¹* mutant flies with spores only promoted the repression of *Defensin* 24 h post-feeding (Fig. 6c). Notably, the global relative levels of *AMP* expression upon spore ingestion were higher in *Dif¹* than in *Rel^{E20}* (compare Figs. 6c and 5d), likely explaining why the bacterial load was reduced in *Dif¹* mutant (Fig. 6a) but not in *Rel^{E20}* (Fig. 5b). While *amidases* were all induced in a WT background upon spore ingestion (Fig. 4a), in the absence of Dif, only *PGRP-LB* remained inducible 24 h post-feeding (Fig. 6d). In *Myd88* mutant flies fed with spores, we observed an induction of the 3 *AMPs* 4 h post ingestion (Fig. 6e) in correlation with the reduced bacterial load reported in Fig. 6a. This result also pinpoints a role of Toll/Myd88 in repressing *AMP* expression in WT background (Fig. 3e). Interestingly, all *amidases* were induced 24 h post spore-feeding (Fig. 6f) suggesting that Toll/Myd88 signaling is not involved in *amidases* upregulation upon spore ingestion.

Dif cooperates with Relish to modulate the intestinal immune response to spore ingestion

To confirm the cooperation of both immune signaling and their downstream NF- κ B transcription factors in regulating the expression of *amidases* and *AMPs* in the posterior midgut, we generated a *Dif¹; Rel^{E20}* double mutant flies. We first monitored *Btk* persistence upon spore ingestion in this genetic background. *Dif¹; Rel^{E20}* double mutant and WT flies ingested a similar amount of spores during the 30 min of feeding (Fig. 7a). However, 120 h later there was a significantly higher *Btk* SA-11 load in the double mutant flies compared with WT (Fig. 7a). Consistently, 6 h after ingestion of *Btk* SA-11^{R/G} spores, more fluorescent bacteria were present in the posterior midguts of *Dif¹; Rel^{E20}* double mutant flies compared with WT (Fig. 7b). In this double mutant background and in absence of spore feeding, the expressions of *AMPs* were lowered (Fig. S7a) suggesting that Dif and Relish act as cofactors to maintain basal levels of *DptA* and *Defensin* expressions while Dif and Relish act redundantly to maintain the basal level of *AttD* expression (Figs. S5a, S6a, and S7a). Our analyses of *amidases* expression in absence of spores revealed that while both factors act as cofactors to maintain the basal expression of *PGRP-SCI*, Relish was required to repress *PGRP-SC2* but Dif appears necessary for *PGRP-SC2* upregulation in absence of Relish (Figs. S5b, S6b, and S7b). Finally, *PGRP-LB* was only regulated by Relish since its expression in the *Dif¹; Rel^{E20}* double mutant was similar to the *Rel^{E20}* single mutant (Figs. S5b and S7b).

Upon spore ingestion, in the *Dif¹; Rel^{E20}* double mutant, the overall levels of *AMP* expression were still low with no repression observed (Fig. 7c). These low levels of *AMPs* correlated with the increased bacterial load observed (Fig. 7a). The expressions of *amidases* were also



not upregulated in the *Dif*¹; *Rel*^{E20} double mutant (Figs. 7d and 4a) confirming that Rel and Dif were necessary together for *PGRP-SC1* induction while only Rel was required for *PGRP-LB* induction and Dif for *PGRPSC-2* induction (Figs. 5e, 6e, and 7d). Overall, these results demonstrate that Dif and Relish cooperate to tightly balance the expression of AMPs and amidases in the posterior midgut of unchallenged as well spore-fed flies.

Discussion

The majority of *Bc*-dependent FBOs, is due to the ingestion of *Bc* bacteria, which must grow in the gut and subsequently produce pore-forming enterotoxins responsible for the onset of diarrhea symptoms¹⁶. However, the mechanisms by which *Bc* bacteria colonize the gut and produce toxins remain poorly understood, and several questions unanswered. Is the disease due to the ingestion of vegetative

Fig. 5 | Imd pathway components are involved in *Bt* persistence. **a, b** SA-11 bacterial load in midguts of different genotypes for components of the Imd pathway 0.5 or 120 h after acute feeding with spores. **a** Homozygous loss of function mutants for *PGRP-LE*^{E12}, *PGRP-LC*^Δ, *Imd*^{shaddock} or *Dredd*⁶⁴. **b** Homozygous loss of function mutant for *RelE*²⁰ or double homozygous loss of function mutant for *PGRP-SC1/2*^Δ; *RelE20*. Silenced (*Rel*^{RNAi}) or overexpressed (*Rel*^{VP16}) Relish in enterocytes (using the *myo1A*^Δ driver). The horizontal axis indicates the mean number of CFUs per midgut. Each dot corresponds to an independent biological replicate where each replicate is the mean of five midguts. **c** Representative confocal images showing SA-11^{RG} spore germination in the anterior and posterior midgut of WT flies (*Canton S*) and *RelE*²⁰ mutant flies 6 h after acute feeding with spores. DAPI (blue)

marks the nuclei. Spores are in red, vegetative cells in green. The yellow fluorescence corresponds to germinating spores (see Fig. 2a). **d–g** RT-qPCR analyses of the expression of AMPs (**d** and **f**) and amidases (**e** and **g**) in *RelE*²⁰ (**d** and **f**) and *PGRP-LE*^{E12} (**e** and **g**) mutant flies 4 h and 24 h after acute feeding with SA-11 spores. UC corresponds to flies fed with water. The dots correspond to independent experiments of 10 pooled female flies. RT-qPCR are represented as relative level of expression normalized to *RP49* and *Dp1* genes. Error bars represent SEM. Two-sided Mann–Whitney test was used to analyze data in **a** and **b**. Two-sided Student's *t* tests were used to analyze data in **d–g**. **p* ≤ 0.05, ***p* ≤ 0.01, ****p* ≤ 0.001, ns non-significant (*P* values are provided in the source data file). Source data are provided as a Source Data file.

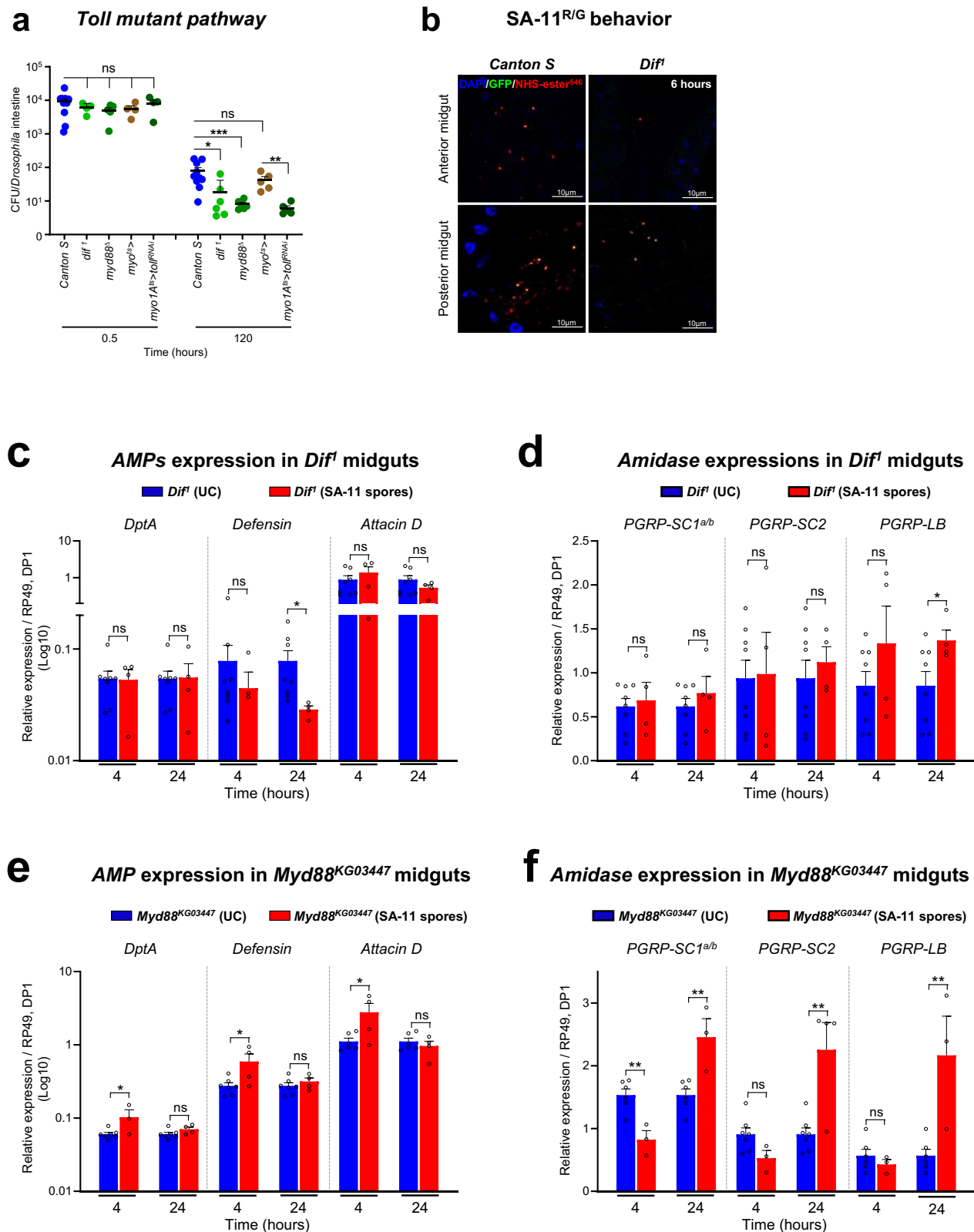
bacteria or spores? What is the distribution and the fate of ingested spores along the gastrointestinal tract? How does the intestinal innate immune system detect and fight the infection? Here, we deciphered the behavior and fate of *Bc* cells in the intestine of *Drosophila melanogaster* and demonstrated that spores escape the innate immune system to reach the posterior part of the midgut/small intestine, where they can germinate and persist for days (Fig. 7e).

First of all, our findings confirm in vivo that after ingestion of vegetative cells, the *Bc* load in the *Drosophila* intestine remains low and that the bacteria are cleared in less than 24 h^{4,52,53}. In *Drosophila*, it has also been shown that the presence of vegetative cells in the anterior midgut is rapidly detected, triggering the production of ROS and visceral spasms, both cooperating to quickly evict the undesired bacteria⁴. Therefore, the minimum infectious dose required to cause intestinal disorders (at least 10⁵ CFU²²;) is likely difficult to reach upon ingestion of vegetative cells. On the contrary, it has been suggested that the capacity of spores to withstand extreme conditions would allow them to overcome stomach acidity and bile salt attacks in the duodenum, favoring germination in the posterior small intestine. Consequently, the infectious dose could be more readily achievable, as illustrated by the 10³ spores/g of food that can be associated with FBOs^{19,54}. The spores of all *Bc* group strains we tested persisted up to 10 days post-ingestion. Consistent with our observations, studies have shown that *Bc* can persist at least 18 days in the intestine of rats transplanted with human-flora⁵⁵ and 30 days in mouse intestine⁵⁶. Moreover *Bt* could be detected in fecal samples in greenhouse workers five days after cessation of bioinsecticide use⁵⁷. Interestingly, we also showed in vivo that spores accumulate and germinate (except for the *Bc* Bactisubtil strain) in the posterior part of the *Drosophila* midgut. Similarly, data suggest that spores derived from the probiotic *B. subtilis* germinate in the jejunum and eventually in the ileum of mice^{58,59}. Our data also highlight the very rapid germination of spores in the posterior parts of the intestine (in less than 2 h). Indeed, while the proximal regions of the *Drosophila* midgut is quite acidic and produce digestive enzymes to break down food, the more distal parts of the intestine harbor a more basic and anaerobic environment with nutrient availability^{35,60,61}. Interestingly, it has been shown, in vitro, that anaerobic conditions slow down the growth rate of *Bc* but favor the production of CytK, Nhe, and Hbl enterotoxins^{16,22,62–66}. Hence, all the conditions for spore germination and enterotoxin production are encountered in the posterior *Drosophila* midgut, which accounts for the occurrence of diarrhetic symptoms when a critical bacterial load is reached. However, contrary to what it has been observed for the *B. subtilis* probiotic strain that can proliferate in the intestine with an intestinal bacterial load either maintained or increasing over a short period^{58,59}, we never observed such an event with the different *Bc/Bt* strains studied, even with the *Bc* Bactisubtil probiotic strain. Moreover, in all our microscopic confocal observations, we did not detect dividing bacteria. Hence, the capacity of probiotic strains to proliferate could be one important feature allowing their establishment in the intestine and the manifestation of their beneficial effects.

Importantly, our data also show that the local innate immune response is ineffective in eliminating vegetative cells in the posterior

regions of the *Drosophila* midgut, which enables *Bc/Bt* persistence. Using *Drosophila* genetic tools, we first show that spores are not detected in the anterior midgut, unlike vegetative cells, which rapidly trigger immune ROS production^{4,36}. Strikingly, although spores germinate in the posterior midgut, there is no release of immune ROS. Immune ROS are normally produced in a DUOX-dependent manner in response to uracil secretion by allochthonous bacteria³⁶. Uracil is thought to serve as bacterial growth factor, promoting proliferation⁶⁷. Hence, we can assume that either *Bc/Bt* vegetative cells in the posterior midgut do not produce uracil or the host receptor for uracil⁶⁸ is absent from the posterior midgut. Moreover, the germination of spores in the posterior midgut, through the activation of the negative regulators, amidases, dampens the production of AMPs. Interestingly, repression of AMP expression was observed in lepidopteran larvae fed with commercial spores of *Bt*⁶⁹ or with spores of *Bt* HD73 strain⁷⁰ suggesting a conserved mechanism, at least in insects. Consequently, the combination of the absence of ROS and the reduced levels of AMPs favor *Bc/Bt* persistence.

Why does spore germination in the posterior midgut induce only genes encoding amidases and not those encoding AMPs? It has been shown that the Imd pathway cytosolic receptor PGRP-LE is required in the anterior midgut to activate AMP genes in response to pathogenic bacteria and to upregulate the amidases PGRP-SC1 and -LB in the posterior midgut in response to commensal bacteria. The transmembrane PGRP-LC receptor is also required in cooperation with PGRP-LE in the anterior midgut to activate the expression of AMPs in response to pathogenic bacteria, however, PGRP-LC is dispensable in the posterior midgut^{5,11,34,45,71–73}. Consistent with this observation, we found that only PGRP-LE is involved in response to spore ingestion and local germination in the posterior midgut. Therefore, in the posterior midgut, the germination of spores allows the activation of the Imd pathway in a PGRP-LE-dependent manner, leading to the induction of three amidases (including *PGRP-SC2*) but not of AMPs. Noteworthy, many convergent data suggest that only amidase genes are inducible in a PGRP-LE-dependent manner in the posterior midgut while AMPs are poorly inducible^{5,11,12,40}. Hence the germination of spores of *Bc/Bt* in the posterior compartment are perceived as if they were commensal bacteria, inducing a tolerance response^{5,74,75} through the induction of amidases that in turn dampen AMPs expression. Our spore ingestion paradigm also reveals that when the Imd pathway is only mobilized in the posterior midgut (spores are not detected in the anterior compartment) in a PGRP-LE-dependent manner, the only response elicited is the induction of amidases, even if the ingested bacteria are non-commensal ones. Consistently, the transcription repressor Caudal and the negative Imd regulator Pirk have been shown to be involved in the repression of AMP expression specifically in the posterior midgut^{5,12,76}. Hence the midgut could be separated into two distinct immune domains: the anterior midgut is competent to fight pathogenic bacteria ingested along with the food, and the posterior midgut is immune-tolerant to sustain commensal flora. *Bc/Bt* spores have developed a strategy to hijack this physiological state for their own benefit, allowing them to escape the strong anterior immune response that would otherwise kill the germinated cells. Consistent with this model, it has been well demonstrated that the *Drosophila* posterior



midgut is capable of increased cell turnover, when compared to the anterior midgut, in order to overcome the damages caused by pathogens^{35,77–80}, likely to compensate for a weaker innate immune response.

Importantly, we cannot compare what we observe in this work using spore feeding for 30 min with all the previous data published using continuous feeding with more elevated doses of vegetative

bacteria. In this latter case, most of the immune events occur in the anterior midgut^{2,81} while with spores that germinate in the posterior midgut, almost nothing happens in the anterior midgut. Our spore paradigm is similar to that of commensal vegetative bacteria, which do not trigger an immune response in the anterior midgut, but induce amidases in the posterior midgut to allow their tolerance by the host^{5,11,72,82}.

Fig. 6 | The Toll pathway is involved in *Bt* persistence. **a** SA-11 bacterial load in midguts of *Dif*^{fl} or *Myd88*^{ΔG0347} homozygous loss of function mutant, or in midguts silenced for Toll (*Toll*^{RNAi}) in enterocytes (using the *myo1A*^{ES} driver) 0.5 or 120 h after acute feeding with spores. The horizontal axis indicates the mean number of CFUs per midgut. Each dot corresponds to an independent biological replicate where each replicate is the mean of five midguts. **b** Representative confocal images showing SA-11^{RG} spore germination in the anterior and posterior midgut of WT flies (*Canton S*) and *Dif*^{fl} homozygous mutant flies 6 h after acute feeding with spores. DAPI (blue) marks the nuclei. Spores are in red, vegetative cells in green. The yellow fluorescence

corresponds to germinating spores (Fig. 2a). **c–f** RT-qPCR analyses of the expression of AMPs (**c** and **e**) and amidases (**d** and **f**) in *Dif*^{fl} (**c** and **d**) or *Myd88*^{ΔG0347} (**e** and **f**) homozygous mutant flies 4 and 24 h after acute feeding with SA-11 spores. Unchallenged flies (UC) corresponds to flies fed with water. The dots correspond to independent experiments of 10 pooled midguts. Error bars represent mean ± SEM of at least three independent experiments. Two-sided Mann–Whitney test was used to analyze data in A. Two-sided Student's *t* tests were used to analyze data in **c–f**. **p* ≤ 0.05, ***p* ≤ 0.01, ****p* ≤ 0.001, ns non-significant (*P* values are provided in the source data file). Source data are provided as a Source Data file.

Unexpectedly, our work in *Drosophila* also revealed that Imd is not the sole signaling pathway driving the innate immune response in the posterior midgut. Indeed it has been well demonstrated that Relish is absolutely required in the anterior midgut downstream of the Imd pathway to mount an efficient immune response against pathogens^{5,8,83,84}. Interestingly, we observed that in the absence of *PGRP-LE* and consequently in absence of *amidases* induction, the AMPs were induced upon the germination of spores. This suggests the existence of an alternative pathway that can trigger the induction of AMPs in response to vegetative bacteria in the posterior midgut. We show that in the posterior midgut, *Dif* intervenes to control *DptA* and *Defensin* activation, probably in cooperation with Relish, since the absence of one of the NF-κB factors is sufficient to shut down their expression. In agreement, it has been shown that during the systemic immune response, both NF-κB factors were able to form hetero- and homodimers to differentially control AMP genes^{75,85–87}. Similarly, Relish and *Dif* likely cooperate to activate *PGRP-SCI*, since its expression is reduced in either *Dif* or *Rel* loss-of-function mutants. Interestingly, Relish and *Dif* appears to act redundantly to control *AttD* expression since both have to be removed to observe its downregulation. Finally, the induction of *PGRP-LB* appears to be only under the control of Relish, and *Dif* and Relish exert opposite effects on *PGRP-SC2* expression. While *Rel* represses its expression, *Dif* is required for its induction upon spore feeding. Interestingly, it has been shown that the IκB factor Pickle can bind to Relish homodimers, converting them into transcriptional repressors of *AttD* expression⁷⁵. Therefore, a combination of NF-κB homo- and hetero-dimers, plus the presence of specific negative regulators, fine-tune the posterior immune response, limiting the level of expression of AMPs to enable commensal flora to become established, but also unfortunately allowing some opportunistic bacteria to persist. Interestingly, a role for *Dif* in shaping the intestinal commensal flora, downstream of the Toll pathway, has recently been uncovered⁸⁸. Along with our results, this suggests that the Toll pathway is also active in the posterior midgut to contribute to the immune response against pathogens.

Together, our data shed light on the conserved behavior and strategy of *Bc/Bt* spores to escape the innate immune response in the proximal part of the intestine, allowing them to reach and germinate in the distal region. Our work also provides useful tools for further investigation to understand when and how enterotoxins are produced and trigger diarrheic symptoms. Our work also highlights that the persistence and load of *Bc/Bt* can be enhanced and could potentially lead to more severe symptoms in immunocompromised individuals.

Methods

Bacterial strains

The two bioinsecticide strains (SA-11 and ABTS-351) were used as commercial formulations. In parallel, the strain ABTS-351 was also used after bacterial isolation and “home-made” spore production as described below. The *Btk*^{ΔCry} (#4D22) and *Bc* Bactisubtil (#6A8, also written Bactisubtyl) strains were collected from the Bacillus Genetics Stock Center (www.bgsc.org)^{31,89}. The *Bc* (#ATCC 14579) was provided by ANSES Maisons-Alfort. *B. toyonensis* strain were selected in this work. *Erwinia carotovora carotovora 15 (Ecc 15)* was kindly provided by

Bruno Lemaître⁹⁰. Bacterial strains were grown in LB medium at 30 °C for 16 h.

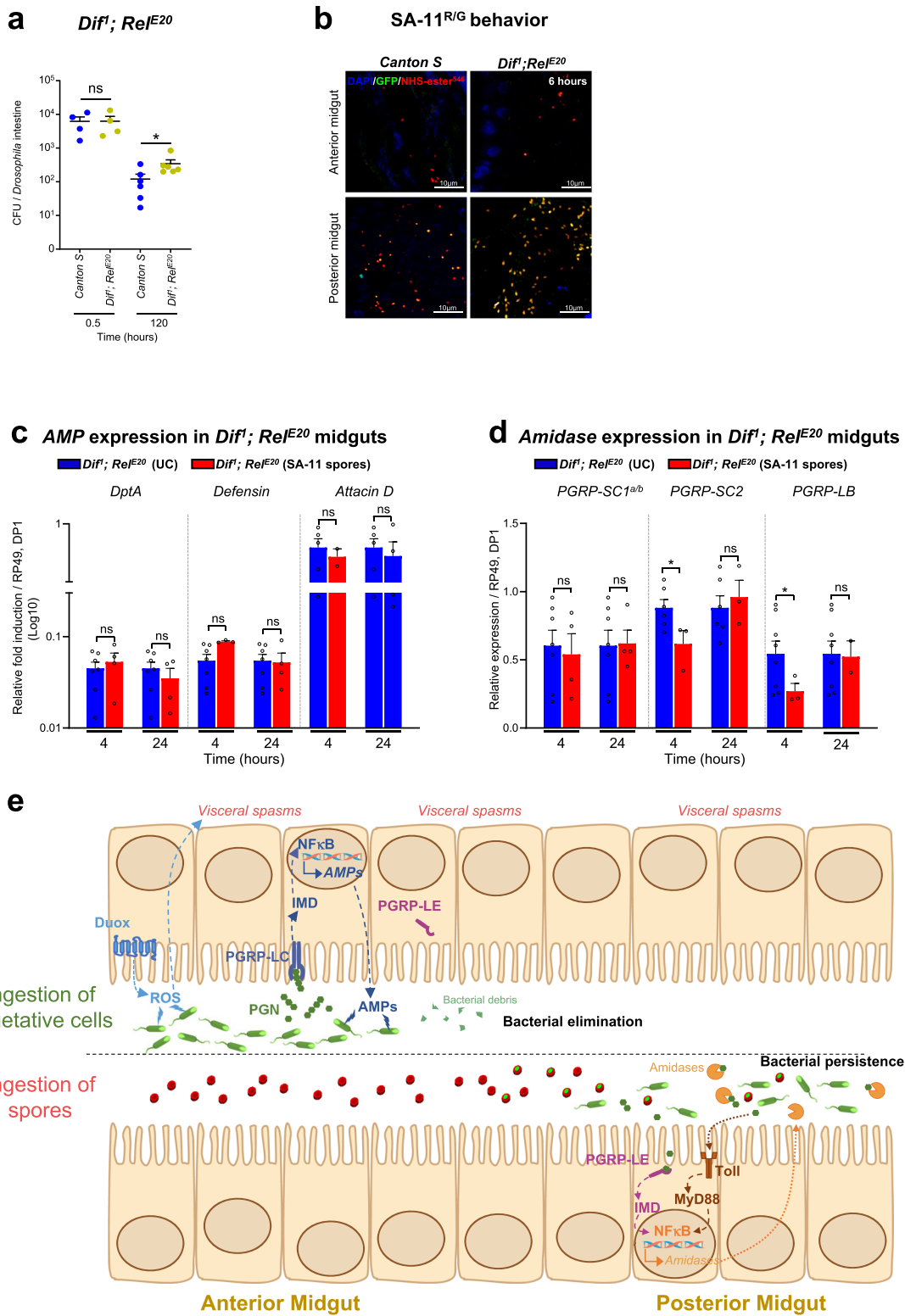
Construction of SA-11^{ΔCry}

The mutant SA-11^{ΔCry} was obtained from the WT strain SA-11, by a procedure of plasmid curing, as follows. After isolation on TSA-YE agar (Biomérieux, 18 h culture at 30 °C), the strain SA-11 was sub-cultured successively 3 times in 10 ml of brain-heart Infusion (BHI, Oxoid) broth at 42 °C with agitation, for 64, 48 and 36 h respectively. The first BHI culture was inoculated from an isolated colony, and the subsequent cultures were inoculated with 100 μl of the previous ones. Clones from the last culture were isolated on TSA-YE agar after serial dilution, then subcultured on the sporulating medium hydrolysate of casein tryptone (HCT) + 0.3% Glc, to select clones unable to produce crystals visible by phase contrast microscopy. The absence of plasmids carrying the *cry* genes was checked by sequencing. Briefly, the genomic DNA of SA-11^{ΔCry} and SA-11 WT were extracted using the KingFisher cell and Tissue DNA kit (ThermoFisher) and sequenced with Illumina technology at the Institut du Cerveau et de la Moelle Epinière (ICM) platform, as previously described¹⁹, (NCBI accession number: SAMN23436137 and SAMN23455549, respectively). The absence of *cry* genes in SA-11^{ΔCry} has been confirmed from raw reads, using KMA⁹¹. Consistently, a plasmid reconstruction made with Mob-Suite⁹² suggested the loss of 4 plasmids in SA-11^{ΔCry} compared with SA-11 WT.

Btk^{ΔCry-GFP}, SA-11^{GFP}, SA-11^{ΔCryGFP}, *Bc*^{GFP}, *Bc* Bactisubtil^{GFP}, and *B. toyonensis*^{GFP} strains

The GFP coding sequence was inserted into the *pHT315* plasmid (bearing the erythromycin-resistant gene)⁹³ (gift from Didier Lereclus). The *pHT315-GFP* recombinant plasmid was transfected and amplified into competent *dam/dcm* *E. Coli* (NEB#C2529H) which allowed it to be demethylated. *pHT315-GFP* was then extracted and purified using either the Pureyield plasmid miniprep kit (Promega #A1223) or the QIAGEN® Plasmid Mini Kit (QIAGEN). For the extraction using the QIAGEN® Plasmid mini Kit, the DNA solution was concentrated by isopropanol precipitation following the manufacturer's recommendations and resuspended in PCR-grade water. The DNA concentrations were measured using the NanoDrop1000 spectrophotometer (Thermo Fisher Scientific).

The different strains from the *Bc* group were transfected with the *pHT315-GFP* plasmid as follows. Strains were plated on TSA-YE agar at room temperature for 48 h, then subcultured in 10 ml of BHI for 18 h at 30 °C, after inoculation from isolated colonies. The cultures were diluted 1/100 in 100 ml BHI and incubated at 37 °C under agitation until an OD_{600nm} of about 0.3 was reached. Bacteria were washed in 10 ml of cold electroporation buffer (400 mM sucrose, 1 mM MgCl₂, phosphate-buffered saline 1X, pH 6.8) and then resuspended in 850 μl of cold electroporation buffer. A hundred μl of each suspension was incubated with 250 ng of plasmid DNA in ice for 5 min, then submitted to electroporation using the MicroPulser Electroporator (Biorad, program Sta), and 2 mm electroporation cuvettes. After the addition of 0.9 ml of BHI, bacteria were incubated for 2 h at 37 °C and isolated on TSA-YE agar supplemented with 10 μg/ml of erythromycin. The selected clones were checked for the expression of GFP using fluorescence microscopy.



Spore production

Spores were produced as described in details in ref. 94. To summarize, strains were plated on LB-agar plates and grown overnight at 30 °C. Bacteria were grown at 30 °C in HCT-agar medium (pH 7.2) containing per 1L: 5g tryptone (Oxoid), 2g casein hydrolysate (Oxoid), 15g agar, 3g glucose, and salts as previously reported in a sporulation-specific medium. After 10 days of incubation, spores were washed with 0.15% NaCl and heat-treated for 20 min at 70 °C. Then cells were centrifuged at 10,000×g, 8 °C for 20 min. Spores were washed with sterile deionized

water and centrifuged at 10,000×g, 8 °C for 20 min. The supernatant was discarded, and the washing was repeated once. The last pellets were taken up in 10 ml and lyophilized (freeze-drying equipment model: RP2V). The numbers of spores produced were determined by estimating the CFUs on LB plates after serial dilution of lyophilized spores.

NHS-ester-547 spore labeling (spore^{R/G})

Btk^{ΔCry-GFP}/SA-11^{GFP}/SA-11^{ΔCry-GFP}/Bc^{GFP}/B. toyonensis^{GFP}/Bc Bactisubtil^{CFP} spores (with known titer) were resuspended in 500 μl of sterile water

Fig. 7 | Dif and Relish are synergistically involved in *Bt* persistence. **a** SA-11 bacterial load in midguts of *Dif¹;Rel^{E20}* homozygous mutants 0.5 or 120 h after acute feeding with spores. The horizontal axis indicates the mean number of CFUs per midgut. Each dot corresponds to an independent biological replicate where each replicate is the mean of five midguts. **b** Representative confocal images showing SA-11^{R/G} spore germination in the anterior and posterior midgut of WT flies (*Canton S*) and *Dif¹;Rel^{E20}* homozygous mutant flies 6 h after acute feeding with spores. DAPI (blue) marks the nuclei. Spores are in red, vegetative cells in green. The yellow fluorescence corresponds to germinating spores. **c, d** RT-qPCR analyses of the expression of *AMPs* (**c**) and *amidases* (**d**) in *Dif¹;Rel^{E20}* homozygous mutant flies 4 and 24 h after acute feeding with SA-11 spores. UC corresponds to flies fed with water. The dots correspond to independent experiments of 10 pooled female flies. Data represent mean \pm SEM. Two-sided Mann–Whitney test was used to analyze data in **a**. Two-sided Student's *t* tests were used to analyze data in **c** and **d**. **p* \leq 0.05, ***p* \leq 0.01, ****p* \leq 0.001, ns = non-significant (*P* values are provided in the source data

file). Source data are provided as a Source Data file. **e** Bacterial persistence upon ingestion of spores. Upper part: ingestion of vegetative cells triggers the release of ROS in the lumen by the Duox enzyme located in anterior enterocytes. In addition to their bacteriostatic activity, ROS induce visceral spasms that accelerate bacterial clearance. Then, the binding of PGNs to the PGRP-LC transmembrane receptor activates the IMD pathway, leading to the release of AMPs which in turn kill the remaining bacteria. Lower part: ingested spores are not perceived by the anterior midgut. Spores reach the posterior midgut where they encounter favorable conditions for their germination. The release of PGNs by the germinating bacteria stimulates the cytoplasmic PGRP-LE receptor directly and the Toll receptor indirectly. The activated IMD and Toll pathways converge on the NF- κ B factors Relish and Dif, which activate the genes encoding amidases. The secreted amidases, by digesting PGNs, exert a negative feedback on AMPs production in the posterior midgut, favoring bacterial persistence.

and incubated 20 min at 70 °C (to remove any residual germinating or vegetative GFP cells). 10 μ l of 1 mM NHS-ester-547 (Interchim #1H0880) were added and the sample was incubated for 1 h with gentle shaking at 4 °C. After centrifugation at 10,000 \times g, at 4 °C for 10 min, the supernatant was removed and the pellet of spores was washed with 1 ml of cold sterile water. This operation is performed twice. The final pellet was resuspended in the required volume of cold sterile water to get the desired concentration spores/100 μ l.

Time-lapse fluorescence of SA-11^{R/G} spore germination

SA-11^{R/G} spores were placed on 1.5% agarose pads on a microscopy slide and covered with a cover glass. The use of agarose pad allowed for stabilizing spores to be achieved in the microscopy samples. The agarose pads were incubated at 37 °C for 60 min to accelerate spore germination process. The time lapse images were taken once every 5 min for 90 min to avoid bleaching. Images were acquired using the Zeiss LSM 880 microscope equipped with the AiryScan detector.

Drosophila rearing and stocks

Flies were reared on our standard laboratory medium⁹⁵ in 12 h/12 h light/dark cycle-controlled incubators. We used the following stocks: WT *Canton S* (Bloomington #64349); *w¹¹¹⁸* (Bloomington #3605); *w¹¹¹⁸* isogenic (gift from Bruno Lemaître); *Rel^{E20}* (Bloomington #55714); *w*; *PGRP-LC^{ΔE}* (Bloomington #55713); *yw*; *PGRP-LE¹¹²* (Bloomington #33055); *w*; *PGRP-SC^Δ* (Bloomington #55724); *w*; *PGRP-LB^Δ* (Bloomington #55715; gift from B. Charroux); *Dredd^{F6496}* (gift from B. Charroux); *imd^{Shaddock}* (gift from B. Charroux); *w*; *Dif¹* (Bloomington #36559); *Myd88^{KGO3447}* (Bloomington #14091); *ΔAMP14* (gift from B. Lemaître)⁹⁷; *w*; *AttD-Gal4 UAS-cherry* (gift from Leopold Kurz)⁹⁸; *w*; *DptA-cherry* (gift from Leopold Kurz, Bloomington #55706); *UAS-DUOX^{RNAi}* (Bloomington #38907); *UAS-REL^{RNAi}* (Bloomington #33661); *UAS-PGRP-LB^{RNAi}* (Bloomington #67236); *UAS-PGRP-SC2^{RNAi}* (Bloomington #56915); *UAS-Toll^{RNAi}* (Bloomington #35628); *UAS-RelHA-VPI6* (Bloomington #36547); *UAS-PGRP-SC2^{#8}/CyO* (gift from Heinrich Jasper)¹³; *w*; *myo1A-Gal4*; *tubGal80ts UAS-GFP/TM6b* (gift from Nicolas Tapon)⁹⁹. The *w*; *Dif¹*; *Rel^{E20}* homozygous viable double mutant was obtained using classic mendelian genetic crosses. Axenic *Canton S* flies were obtained as described in ref. 95. It should be noted that we did not isogenize flies because we wanted to understand whether the persistence we observed was a general mechanism occurring independently of the genetic background, which is indeed the case.

Drosophila oral intoxication

Five-six-days old virgin females *Drosophila* were reared at 25 °C. For conditional expression of UAS-GAL80^{ts} linked transgenes, flies were developed at room temperature, then shifted to 29 °C for 7 days to induce transgene expression. Before intoxication, *Drosophila* females were put into a new vial without medium for starvation for 2 h at 25 °C

or at 29 °C for UAS-GAL80^{ts} flies. This allows the synchronization of food intake once in contact with the contaminated medium. Ten females were transferred into a *Drosophila* narrow vial containing fly medium covered with a filter disk where the spore solution was deposited. The inoculum used for continuous and acute intoxication were respectively 10⁶ CFU/5 cm²/fly and 10⁸ CFU/5 cm²/fly respectively. For the acute intoxication, *Drosophila* were fed for 30 min with the spore inoculum, then transferred to a new sterile vial until dissection. For the continuous intoxication, *Drosophila* were let in contact with the spore inoculum until the dissection time. For control conditions, *Drosophila* females were fed with sterile deionized water in the same conditions.

Bacterial load quantification (CFU) in *Drosophila* midgut

Flies were washed first in ethanol 70% and then in PBSIX before guts dissection in PBSIX. Five whole midguts or 5 split parts (anterior and posterior regions) were crushed in 200 μ l of LB at various times post-ingestion using a micro pestle and the homogenate was serially diluted in LB and incubated overnight at 30 °C on LB agar plates. Colony counting was performed the day after. Importantly the time point 30 min correspond to the end of the acute feeding and serve as food intake control. In dot graphs, each dot corresponds to 5 intestines. Each experiment (5 midguts/time point) was carried out at least in three independent replicates.

Bacterial load quantification (CFU) on the filter disk

The filter disk was washed and vortexed in 1 ml of sterile water. The homogenate was serially diluted in sterile water and incubated overnight at 30 °C on LB agar plates. Colony counting was performed the day after. Three independent replicates were performed.

Bacterial load quantification (CFU) in feces

After 2 h of starvation followed by 30 min of feeding with the spore inoculum, 10 flies were placed in a new vial containing 5 mL of sterile food and surrounded by filter paper. Then, flies were removed, the filter paper was washed and vortexed in 5 ml of sterile water. The homogenate was serially diluted in sterile water and incubated overnight at 30 °C on LB agar plates. The colony counting was performed the following day. All experiments were conducted at 25 °C. Three independent replicates were performed.

Bacterial load quantification (CFU) on fly body

After acute intoxication, 10 flies were transferred in a new sterile vial. Then 4, 24 or 48 h later, flies were removed from their vial and washed first 20 s in ethanol 70% and then 10 min in PBSIX. After, flies were immersed in 100 μ l of LB and the LB further plated on LB agar plates over night at 30 °C. Three independent replicates were performed.⁷³⁰

Heat treatment

The intestinal samples or the filter disk samples were heated at 75 °C for 25 min to kill the germinating spores and the vegetative cells. Afterward, the spores were enumerated as described above.

In vivo monitoring of spore germination

Flies were fed with *Btk* SA-11^{RG}. Guts were dissected and fixed with 4% formaldehyde in PBSIX for 20 min and immediately mounted in Fluoroshield-DAPI medium. Images acquisition was performed at the microscopy platform of the Institut Sophia Agrobiotech (INRAE 1355-UCA-CNRS 7254-Sophia Antipolis) with the microscope Zeiss Axio-Zoom V16 with an Apotome 2 and a Zeiss LSM 880 microscope equipped with the AiryScan detector. Images were analyzed using ZEN and Photoshop software and ImageJ.

RNA extraction and Real-time qPCR for *Drosophila* guts

At least three biological replicates were independently generated for each condition. Total RNA was extracted from 10 *Drosophila* midguts using Microelute Total RNA kit (Omega Bio Tek) and dissolved in 20 µl of RNase-free water. The quantity and quality of RNA were assessed using a Thermo ScientificTM NanoDrop 2000. 550 ng of extracted RNA was reverse transcribed to cDNA using QscriptTM. Real-time PCR was performed on AriaMX Real-Time (Agilent) in a final volume of 20 µl, using the EvaGreen kit. Three technical replicates were done for each experiment. Relative expression data were normalized to *RP49* and *DpI* genes and calculated according to the delta-delta C_t method¹⁰⁰. All the results were analyzed with geNorm software. In brief, this software allows normalization of each gene expression level against a geometrical mean of the two reference genes, as well as the integration of the technical replicates and amplification efficiencies and associated errors (primer sequences are listed in Table S1).

HOCl staining with R19S

The protocol is described in ref. 38.

Quantification and statistical analysis

Statistical analyses were performed using GraphPad Prism v.7.00 or Microsoft Excel software (Anastats spreadsheet for Mann–Whitney's test, <http://www.anastats.fr>). Data are presented as mean and SEM. For all comparisons throughout our study, we performed two-sided unpaired Non-parametric Mann–Whitney's test or Student's t-tests, as specified on each figure legends. **p* ≤ 0.05, ***p* ≤ 0.01, ****p* ≤ 0.001, ns = non-significant. For the t-tests (RT-qPCR), the exact *P* values are provided in the source data file. Diagrams and figures were produced using PowerPoint.

Reporting summary

Further information on research design is available in the Nature Portfolio Reporting Summary linked to this article.

Data availability

All source data needed to evaluate the conclusions are present in the paper as a Source Data file. Source data are provided with this paper. SAMN23436137 and SAMN23455549 sequences have been deposited at the NCBI and are freely accessible. Source data are provided with this paper.

References

1. Capo, F., Wilson, A. & Di Cara, F. The intestine of *Drosophila* melanogaster: an emerging versatile model system to study intestinal epithelial homeostasis and host-microbial interactions in humans. *Microorganisms* **7**, microorganisms7090336 (2019).
2. Royet, J. & Charroux, B. Mechanisms and consequence of bacteria detection by the *Drosophila* gut epithelium. *Gut* **4**, 259–263 (2013).
3. Kim, S. H. & Lee, W. J. Role of DUOX in gut inflammation: lessons from *Drosophila* model of gut-microbiota interactions. *Front Infect. Microbiol.* **3**, 116 (2014).
4. Benguettat, O. et al. The DH31/CGRP enteroendocrine peptide triggers intestinal contractions favoring the elimination of opportunistic bacteria. *PLoS Pathog.* **14**, e1007279 (2018).
5. Bosco-Drayon, V. et al. Peptidoglycan sensing by the receptor PGRP-LE in the *Drosophila* gut induces immune responses to infectious bacteria and tolerance to microbiota. *Cell Host Microbe* **12**, 153–165 (2012).
6. Kaneko, T. et al. PGRP-LC and PGRP-LE have essential yet distinct functions in the *Drosophila* immune response to monomeric DAP-type peptidoglycan. *Nat. Immunol.* **7**, 715–723 (2006).
7. Bonfini, A., Liu, X. & Buchon, N. From pathogens to microbiota: how *Drosophila* intestinal stem cells react to gut microbes. *Dev. Comp. Immunol.* **64**, 22–38 (2016).
8. Buchon, N., Broderick, N. A., Poidevin, M., Pradervand, S. & Lemaitre, B. *Drosophila* intestinal response to bacterial infection: activation of host defense and stem cell proliferation. *Cell Host Microbe* **5**, 200–211 (2009).
9. Chakrabarti, S., Liehl, P., Buchon, N. & Lemaitre, B. Infection-induced host translational blockage inhibits immune responses and epithelial renewal in the *Drosophila* gut. *Cell Host Microbe* **12**, 60–70 (2012).
10. Zhai, Z., Huang, X. & Yin, Y. Beyond immunity: the Imd pathway as a coordinator of host defense, organismal physiology and behavior. *Dev. Comp. Immunol.* **83**, 51–59 (2018).
11. Costechareyre, D. et al. Tissue-specific regulation of *Drosophila* NF-κB pathway activation by peptidoglycan recognition protein SC. *J. Innate Immun.* **8**, 67–80 (2016).
12. Paredes, J. C., Welchman, D. P., Poidevin, M. & Lemaitre, B. Negative regulation by amidase PGRPs shapes the *Drosophila* antibacterial response and protects the fly from innocuous infection. *Immunity* **35**, 770–779 (2011).
13. Guo, L., Karpac, J., Tran, S. L. & Jasper, H. PGRP-SC2 promotes gut immune homeostasis to limit commensal dysbiosis and extend lifespan. *Cell* **156**, 109–122 (2014).
14. Ehling-Schulz, M., Lereclus, D. & Koehler, T. M. The *Bacillus cereus* group: *Bacillus* species with pathogenic potential. *Microbiol Spectr.* <https://doi.org/10.1128/microbiolspec.GPP3-0032-2018>. (2019).
15. Setlow, P. Spore resistance properties. *Microbiol. Spectr.* <https://doi.org/10.1128/microbiolspec.TBS-0003-2012>. (2014).
16. Jovanovic, J., Ornelis, V. F. M., Madder, A. & Rajkovic, A. *Bacillus cereus* food intoxication and toxicoinfection. *Compr. Rev. Food Sci. Food Saf.* **20**, 3719–3761 (2021).
17. Dietrich, R., Jessberger, N., Ehling-Schulz, M., Märtlbauer, E. & Granum, P. E. The food poisoning toxins of *Bacillus cereus*. *Toxins (Basel)* **13**, 98 (2021).
18. Santé publique France. <https://www.santepubliquefrance.fr/>. (2024).
19. Bonis, M. et al. Comparative phenotypic, genotypic and genomic analyses of *Bacillus thuringiensis* associated with foodborne outbreaks in France. *PLoS ONE* **16**, e0246885 (2021).
20. Glasset, B. et al. *Bacillus cereus*-induced food-borne outbreaks in France, 2007 to 2014: epidemiology and genetic characterisation. *Eur. Surveill.* **21**, 30413 (2016).
21. EFSA & ECDC. The European Union One Health 2022 Zoonoses Report. *EFSA J.* **21**, e8442 (2023).
22. Berthold-Pluta, A., Pluta, A. & Garbowska, M. The effect of selected factors on the survival of *Bacillus cereus* in the human gastrointestinal tract. *Microb. Pathog.* **82**, 7–14 (2015).

23. Clavel, T., Carlin, F., Lairon, D., Nguyen-The, C. & Schmitt, P. Survival of *Bacillus cereus* spores and vegetative cells in acid media simulating human stomach. *J. Appl. Microbiol.* **97**, 214–219 (2004).
24. Barbosa, T. M., Serra, C. R., La Ragione, R. M., Woodward, M. J. & Henriques, A. O. Screening for bacillus isolates in the broiler gastrointestinal tract. *Appl. Environ. Microbiol.* **71**, 968–978 (2005).
25. Ceuppens, S. et al. Survival and germination of *Bacillus cereus* spores without outgrowth or enterotoxin production during in vitro simulation of gastrointestinal transit. *Appl. Environ. Microbiol.* **78**, 7698–7705 (2012).
26. Ceuppens, S. et al. Survival of *Bacillus cereus* vegetative cells and spores during in vitro simulation of gastric passage. *J. Food Prot.* **75**, 690–694 (2012).
27. Ceuppens, S., Uyttendaele, M., Hamelink, S., Boon, N. & Van de Wiele, T. Inactivation of *Bacillus cereus* vegetative cells by gastric acid and bile during in vitro gastrointestinal transit. *Gut Pathog.* **4**, 11 (2012).
28. Carroll, L. M., Cheng, R. A., Wiedmann, M. & Kovac, J. Keeping up with the *Bacillus cereus* group: taxonomy through the genomics era and beyond. *Crit. Rev. Food Sci. Nutr.* **62**, 1–26 (2021).
29. Carroll, L. M., Wiedmann, M. & Kovac, J. Proposal of a taxonomic nomenclature for the bacillus cereus group which reconciles genomic definitions of bacterial species with clinical and industrial phenotypes. *mBio* **11**, e00034–20 (2020).
30. Ivanova, N. et al. Genome sequence of *Bacillus cereus* and comparative analysis with *Bacillus anthracis*. *Nature* **423**, 87–91 (2003).
31. Hoa, N. T. et al. Characterization of *Bacillus* species used for oral bacteriotherapy and bacterioprophyllaxis of gastrointestinal disorders. *Appl. Environ. Microbiol.* **66**, 5241–5247 (2000).
32. Johler, S. et al. Enterotoxin production of *Bacillus thuringiensis* isolates from biopesticides, foods, and outbreaks. *Front. Microbiol.* **9**, 1915 (2018).
33. Biggel, M. et al. Whole genome sequencing reveals biopesticidal origin of *Bacillus thuringiensis* in foods. *Front. Microbiol.* **12**, 775669 (2021).
34. Buchon, N. et al. Morphological and molecular characterization of adult midgut compartmentalization in *Drosophila*. *Cell Rep.* **3**, 1725–1738 (2013).
35. Marianes, A. & Spradling, A. C. Physiological and stem cell compartmentalization within the *Drosophila* midgut. *Elife* **2**, e00886 (2013).
36. Lee, K. A. et al. Bacterial-derived uracil as a modulator of mucosal immunity and gut-microbe homeostasis in *Drosophila*. *Cell* **153**, 797–811 (2013).
37. Tzou, P. et al. Tissue-specific inducible expression of antimicrobial peptide genes in *Drosophila* surface epithelia. *Immunity* **13**, 737–748 (2000).
38. Hachfi, S., Benguetat, O. & Gallet, A. Hypochlorous acid staining with R19-S in the *Drosophila* intestine upon ingestion of opportunistic bacteria. *Bio-Protoc.* **9**, e3246 (2019).
39. Chen, X. et al. A specific and sensitive method for detection of hypochlorous acid for the imaging of microbe-induced HOCl production. *Chem. Commun. (Camb.)* **47**, 4373–4375 (2011).
40. Charroux, B. et al. Cytosolic and secreted peptidoglycan-degrading enzymes in *Drosophila* respectively control local and systemic immune responses to microbiota. *Cell Host Microbe* **23**, 215–228.e4 (2018).
41. Hanson, M. A. et al. Synergy and remarkable specificity of antimicrobial peptides in vivo using a systematic knockout approach. *eLife* **8**, e44341 (2019).
42. Carboni, A. L., Hanson, M. A., Lindsay, S. A., Wasserman, S. A. & Lemaitre, B. Cecropins contribute to *Drosophila* host defense against a subset of fungal and Gram-negative bacterial infection. *Genetics* **220**, iyab188 (2022).
43. Hedengren, M. et al. Relish, a central factor in the control of humoral but not cellular immunity in *Drosophila*. *Mol. Cell* **4**, 827–837 (1999).
44. Vodovar, N. et al. *Drosophila* host defense after oral infection by an entomopathogenic *Pseudomonas* species. *Proc. Natl Acad. Sci. USA* **102**, 11414–11419 (2005).
45. Zhai, Z., Boquete, J. P. & Lemaitre, B. Cell-specific Imd-NF-kappaB responses enable simultaneous antibacterial immunity and intestinal epithelial cell shedding upon bacterial infection. *Immunity* **48**, 897–910.e7 (2018).
46. Petersen, U. M., Björklund, G., Ip, Y. T. & Engström, Y. The dorsal-related immunity factor, Dif, is a sequence-specific trans-activator of *Drosophila* Cecropin gene expression. *EMBO J.* **14**, 3146–3158 (1995).
47. Manfrulli, P., Reichhart, J. M., Steward, R., Hoffmann, J. A. & Lemaitre, B. A mosaic analysis in *Drosophila* fat body cells of the control of antimicrobial peptide genes by the Rel proteins Dorsal and DIF. *EMBO J.* **18**, 3380–3391 (1999).
48. Rosetto, M., Engström, Y., Baldari, C. T., Telford, J. L. & Hultmark, D. Signals from the IL-1 receptor homolog, Toll, can activate an immune response in a *Drosophila* hemocyte cell line. *Biochem Biophys. Res. Commun.* **209**, 111–116 (1995).
49. Meng, X., Khanuja, B. S. & Ip, Y. T. Toll receptor-mediated *Drosophila* immune response requires Dif, an NF-kappaB factor. *Genes Dev.* **13**, 792–797 (1999).
50. Tauszig-Delamasure, S., Bilak, H., Capovilla, M., Hoffmann, J. A. & Imler, J. L. *Drosophila* MyD88 is required for the response to fungal and Gram-positive bacterial infections. *Nat. Immunol.* **3**, 91–97 (2002).
51. Horng, T. & Medzhitov, R. *Drosophila* MyD88 is an adapter in the Toll signaling pathway. *Proc. Natl Acad. Sci. USA* **98**, 12654–12658 (2001).
52. Rolny, I. S., Minnaard, J., Racedo, S. M. & Pérez, P. F. Murine model of *Bacillus cereus* gastrointestinal infection. *J. Med. Microbiol.* **63**, 1741–1749 (2014).
53. Loudhaief, R. et al. Apoptosis restores cellular density by eliminating a physiologically or genetically induced excess of enterocytes in the *Drosophila* midgut. *Development* **144**, 808–819 (2017).
54. EFSA BIOHAZ. Risks for public health related to the presence of *Bacillus cereus* and other *Bacillus* spp. including *Bacillus thuringiensis* in foodstuffs. *EFSA J.* **14**, e04524 (2016).
55. Wilcks, A. et al. Germination and conjugation of *Bacillus thuringiensis* subsp. *israelensis* in the intestine of gnotobiotic rats. *J. Appl. Microbiol.* **104**, 1252–1259 (2008).
56. Oliveira-Filho, E. C. et al. Toxicity assessment and clearance of Brazilian microbial pest control agents in mice. *Bull. Environ. Contam. Toxicol.* **83**, 570–574 (2009).
57. Jensen, G. B. et al. *Bacillus thuringiensis* in fecal samples from greenhouse workers after exposure to *B. thuringiensis*-based pesticides. *Appl. Environ. Microbiol.* **68**, 4900–4905 (2002).
58. Casula, G. & Cutting, S. M. *Bacillus* probiotics: spore germination in the gastrointestinal tract. *Appl. Environ. Microbiol.* **68**, 2344–2352 (2002).
59. Tam, N. K. et al. The intestinal life cycle of *Bacillus subtilis* and close relatives. *J. Bacteriol.* **188**, 2692–2700 (2006).
60. Osman, D. et al. Autocrine and paracrine unpaired signaling regulate intestinal stem cell maintenance and division. *J. Cell Sci.* **125**, 5944–5949 (2012).
61. Shanbhag, S. & Tripathi, S. Epithelial ultrastructure and cellular mechanisms of acid and base transport in the *Drosophila* midgut. *J. Exp. Biol.* **212**, 1731–1744 (2009).
62. Dupont, C., Zigha, A., Rosenfeld, E. & Schmitt, P. Control of enterotoxin gene expression in *Bacillus cereus* F4430/73 involves

- the redox-sensitive ResDE signal transduction system. *J. Bacteriol.* **188**, 6640–6651 (2006).
63. Duport, C., Thomassin, S., Bourel, G. & Schmitt, P. Anaerobiosis and low specific growth rates enhance hemolysin BL production by *Bacillus cereus* F4430/73. *Arch. Microbiol.* **182**, 90–95 (2004).
64. Zigha, A., Rosenfeld, E., Schmitt, P. & Duport, C. Anaerobic cells of *Bacillus cereus* F4430/73 respond to low oxidoreduction potential by metabolic readjustments and activation of enterotoxin expression. *Arch. Microbiol.* **185**, 222–233 (2006).
65. van der Voort, M. & Abee, T. Transcriptional regulation of metabolic pathways, alternative respiration and enterotoxin genes in anaerobic growth of *Bacillus cereus* ATCC 14579. *J. Appl. Microbiol.* **107**, 795–804 (2009).
66. Miller, B. M., Liou, M. J., Lee, J. Y. & Bäuml, A. J. The longitudinal and cross-sectional heterogeneity of the intestinal microbiota. *Curr. Opin. Microbiol.* **63**, 221–230 (2021).
67. Du, E. J. et al. TrpA1 regulates defecation of food-borne pathogens under the control of the duox pathway. *PLoS Genet.* **12**, e1005773 (2016).
68. Lee, K. A. et al. Bacterial uracil modulates *Drosophila* DUOX-dependent gut immunity via hedgehog-induced signaling endosomes. *Cell Host Microbe* **17**, 191–204 (2015).
69. Tamez-Guerra, P. et al. Detection of genes encoding antimicrobial peptides in Mexican strains of *Trichoplusia ni* (Hübner) exposed to *Bacillus thuringiensis*. *J. Invertebr. Pathol.* **98**, 218–227 (2008).
70. Li, S. et al. *Bacillus thuringiensis* suppresses the humoral immune system to overcome defense mechanism of *Plutella xylostella*. *Front. Physiol.* **9**, 1478 (2018).
71. Neyen, C., Poidevin, M., Roussel, A. & Lemaitre, B. Tissue- and ligand-specific sensing of gram-negative infection in *Drosophila* by PGRP-LC isoforms and PGRP-LE. *J. Immunol.* **189**, 1886–1897 (2012).
72. Onuma, T. et al. Recognition of commensal bacterial peptidoglycans defines *Drosophila* gut homeostasis and lifespan. *PLoS Genet.* **19**, e1010709 (2023).
73. Rodgers, F. H. et al. Functional analysis of the three major PGRP-LC isoforms in the midgut of the malaria mosquito *Anopheles coluzzii*. *Insect Biochem. Mol. Biol.* **118**, 103288 (2020).
74. Bonnay, F. et al. big bang gene modulates gut immune tolerance in *Drosophila*. *Proc. Natl Acad. Sci. USA* **110**, 2957–2962 (2013).
75. Morris, O. et al. Signal integration by the I κ B protein pickle shapes *Drosophila* innate host defense. *Cell Host Microbe* **20**, 283–295 (2016).
76. Ryu, J. H. et al. Innate immune homeostasis by the homeobox gene *caudal* and commensal-gut mutualism in *Drosophila*. *Science* **319**, 777–782 (2008).
77. Apidianakis, Y., Pitsouli, C., Perrimon, N. & Rahme, L. Synergy between bacterial infection and genetic predisposition in intestinal dysplasia. *Proc. Natl Acad. Sci. USA* **106**, 20883–20888 (2009).
78. Jiang, H. et al. Cytokine/Jak/Stat signaling mediates regeneration and homeostasis in the *Drosophila* midgut. *Cell* **137**, 1343–1355 (2009).
79. Zhou, F., Rasmussen, A., Lee, S. & Agaisse, H. The UPD3 cytokine couples environmental challenge and intestinal stem cell division through modulation of JAK/STAT signaling in the stem cell microenvironment. *Dev. Biol.* **373**, 383–393 (2013).
80. Tamamouna, V. et al. Evidence of two types of balance between stem cell mitosis and enterocyte nucleus growth in the *Drosophila* midgut. *Development* **147**, dev189472 (2020).
81. Ferguson, M. & Foley, E. Microbial recognition regulates intestinal epithelial growth in homeostasis and disease. *FEBS J.* **289**, 3666–3691 (2022).
82. Broderick, N. A., Buchon, N. & Lemaitre, B. Microbiota-induced changes in *Drosophila melanogaster* host gene expression and gut morphology. *MBio* **5**, e01117–14 (2014).
83. Buchon, N., Broderick, N. A., Chakrabarti, S. & Lemaitre, B. Invasive and indigenous microbiota impact intestinal stem cell activity through multiple pathways in *Drosophila*. *Genes Dev.* **23**, 2333–2344 (2009).
84. Cronin, S. J. et al. Genome-wide RNAi screen identifies genes involved in intestinal pathogenic bacterial infection. *Science* **325**, 340–343 (2009).
85. Han, Z. S. & Ip, Y. T. Interaction and specificity of Rel-related proteins in regulating *Drosophila* immunity gene expression. *J. Biol. Chem.* **274**, 21355–21361 (1999).
86. Tanji, T., Yun, E. Y. & Ip, Y. T. Heterodimers of NF- κ B transcription factors DIF and Relish regulate antimicrobial peptide genes in *Drosophila*. *Proc. Natl Acad. Sci. USA* **107**, 14715–14720 (2010).
87. Chowdhury, M. et al. An in vitro study of NF- κ B factors cooperatively in regulation of *Drosophila melanogaster* antimicrobial peptide genes. *Dev. Comp. Immunol.* **95**, 50–58 (2019).
88. Bahuguna, S. et al. Bacterial recognition by PGRP-SA and downstream signalling by Toll/DIF sustain commensal gut bacteria in *Drosophila*. *PLoS Genet.* **18**, e1009992 (2022).
89. Gonzalez, J. M. Jr., Brown, B. J. & Carlton, B. C. Transfer of *Bacillus thuringiensis* plasmids coding for delta-endotoxin among strains of *B. thuringiensis* and *B. cereus*. *Proc. Natl Acad. Sci. USA* **79**, 6951–6955 (1982).
90. Basset, A. et al. The phytopathogenic bacteria *Erwinia carotovora* infects *Drosophila* and activates an immune response. *Proc. Natl Acad. Sci. USA* **97**, 3376–3381 (2000).
91. Clausen, P., Aarestrup, F. M. & Lund, O. Rapid and precise alignment of raw reads against redundant databases with KMA. *BMC Bioinform.* **19**, 307 (2018).
92. Robertson, J. & Nash, J. H. E. MOB-suite: software tools for clustering, reconstruction and typing of plasmids from draft assemblies. *Microb. Genom.* **4**, e000206 (2018).
93. Theodulou, C., Vega, A., Salazar, M., González, E. & Meza-Basso, L. Expression of a *Bacillus thuringiensis* delta-endotoxin cry1Ab gene in *Bacillus subtilis* and *Bacillus licheniformis* strains that naturally colonize the phylloplane of tomato plants (*Lycopersicon esculentum*, Mills). *J. Appl. Microbiol.* **94**, 375–381 (2003).
94. Fichant, A. et al. New approach methods to assess the enteropathogenic potential of strains of the *Bacillus cereus* group, including *Bacillus thuringiensis*. *Foods* **13**, 1140 (2024).
95. Nawrot-Espósito, M. P. et al. *Bacillus thuringiensis* bioinsecticides induce developmental defects in non-target *Drosophila melanogaster* larvae. *Insects* **11**, 697 (2020).
96. Leulier, F., Rodriguez, A., Khush, R. S., Abrams, J. M. & Lemaitre, B. The *Drosophila* caspase Dredd is required to resist gram-negative bacterial infection. *EMBO Rep.* **1**, 353–358 (2000).
97. Carboni, A. L., Hanson, M. A., Lindsay, S. A., Wasserman, S. A. & Lemaitre, B. Cecropins contribute to *Drosophila* host defense against a subset of fungal and Gram-negative bacterial infection. *Genetics* **220**, iyab188 (2022).
98. Tavignot, R., Chaduli, D., Djitte, F., Charroux, B. & Royet, J. Inhibition of a NF- κ B/Diap1 pathway by PGRP-LF is required for proper apoptosis during *Drosophila* development. *PLoS Genet.* **13**, e1006569 (2017).
99. Shaw, R. L. et al. The Hippo pathway regulates intestinal stem cell proliferation during *Drosophila* adult midgut regeneration. *Development* **137**, 4147–4158 (2010).
100. Pfaffl, M. W. A new mathematical model for relative quantification in real-time RT-PCR. *Nucleic Acids Res.* **29**, e45 (2001).

Acknowledgements

We would like to thank Bernard Charroux, François Leulier, Julien Royet, Heinrich Jasper, Leopold Kurz, Mark Hanson, Samuel Romme-laere, and Bruno Lemaitre for kindly providing fly stocks. We also thank Didier Lereclus for providing the pHT315 plasmid. We are grateful to Leanne Jones, Raphaël Rousset, Carmelo Luci, and Bernard Charroux for their advice on the project and the manuscript. We especially thank Bruno Lemaitre for the critical reading of the manuscript. We also thank Olivier Pierre and Anne Doye for their help with the microscopy, and Alexia Danné, Audrey Amate, and Olivia Benguettat for their technical help. Our thanks to the Université Côte d'Azur Office of International Scientific Visibility for English language editing of the manuscript. We also thank the Space, Environment, Risk and Resilience Academy of the Université Côte d'Azur for their financial support. This work has been supported by the French government, through the UCAJEDI Investments in the Future project managed by the National Research Agency (ANR) with the reference number ANR-15-IDEX-01 to A.G. and L.B., and through the ANR-13-CESA-0003-01 (ImBio) and the ANR-22-CE35-0006-01 (BaDAss) to A.G. This work has also been supported by the Plan ECOPHYTO II+ Axe 3 - Action 11 under the N°OFB.21.0450 to M.B., by the "Fondation ARC pour la recherche sur le cancer" (20171206145) and by the "Institut Olga Triballat" (AAP2021; institut-olga.triballat.org) to R.Ro., and by the Anses (N°ANSES-22-EST-203) to R.Ru.; A.F. was funded by a PhD grant from INRAE and Anses.

Author contributions

Conceptualization: S.H., L.B. and A.G. Methodology: S.H., A.B.-B., A.F., P.M., M.-P.N.-E., G.M. and M.B. Validation: S.H., A.B.-B., P.M., M.B., L.B. and A.G. Formal Analysis: S.H., A.B.-B., P.M., L.B. and A.G. Investigation: S.H., A.B.-B., A.F., P.M., M.-P.N.-E. and M.B. Data Curation: S.H., A.B.-B., A.F., P.M., M.B., L.B. and A.G. Writing – Original Draft: S.H. and A.G. Writing – Review & Editing: S.H., A.B.-B., R.Ro., M.B., L.B. and A.G. Visualization: S.H., L.B. and A.G. Supervision: L.B. and A.G. Project Administration: L.B. and A.G. Funding Acquisition: M.B., R.Ru., R.Ro., L.B. and A.G.

Competing interests

The authors declare no competing interests.

Additional information

Supplementary information The online version contains supplementary material available at <https://doi.org/10.1038/s41467-024-51689-9>.

Correspondence and requests for materials should be addressed to Laurent Boyer or Armel Gallet.

Peer review information *Nature Communications* thanks Fengliang Jin, Yoshitomo Kikuchi and the other, anonymous, reviewer(s) for their contribution to the peer review of this work. A peer review file is available.

Reprints and permissions information is available at <http://www.nature.com/reprints>

Publisher's note Springer Nature remains neutral with regard to jurisdictional claims in published maps and institutional affiliations.

Open Access This article is licensed under a Creative Commons Attribution-NonCommercial-NoDerivatives 4.0 International License, which permits any non-commercial use, sharing, distribution and reproduction in any medium or format, as long as you give appropriate credit to the original author(s) and the source, provide a link to the Creative Commons licence, and indicate if you modified the licensed material. You do not have permission under this licence to share adapted material derived from this article or parts of it. The images or other third party material in this article are included in the article's Creative Commons licence, unless indicated otherwise in a credit line to the material. If material is not included in the article's Creative Commons licence and your intended use is not permitted by statutory regulation or exceeds the permitted use, you will need to obtain permission directly from the copyright holder. To view a copy of this licence, visit <http://creativecommons.org/licenses/by-nc-nd/4.0/>.

© The Author(s) 2024